SRI International

DVORSCAK

June 1995

DIRECT CATALYTIC CONVERSION OF METHANE AND LIGHT HYDROCARBON GASES

Final Report

Covering the Period October 1, 1986 to July 31, 1989

By: Robert B. Wilson Jr., Barry M. Posin, and Yee-Wai Chan

Prepared for:

U.S. Department of Energy
Pittsburgh Energy Technology Center
P.O. Box 10940
Pittsburgh, PA 15236-0940

Attention: Dr. Udaya S. Rao
Project Manager

Contract No. DE-AC22-86PC90011
SRI Project 2678

333 Ravenswood Avenue ◦ Menlo Park, CA 94025-3493 ◦ (415) 326-6200 ◦ FAX: (415) 326-5512 ◦ Telex: 334486

DOE/PC/90011--T30

June 1995

DIRECT CATALYTIC CONVERSION OF METHANE AND LIGHT HYDROCARBON GASES

Final Report

Covering the Period October 1, 1986 to July 31, 1989

By: Robert B. Wilson Jr., Barry M. Posin, and Yee-Wai Chan

Prepared for:

U.S. Department of Energy
Pittsburgh Energy Technology Center
P.O. Box 10940
Pittsburgh, PA 15236-0940

Attention: Dr. Udaya S. Rao
Project Manager

Contract No. DE-AC22-86PC90011
SRI Project 2678

Approved:

David Ross
Laboratory Director
Chemistry Laboratory

David M. Golden
Senior Vice President
Science and Technology Group

ABSTRACT

This project, which was supported by the U.S. Department of Energy—Pittsburgh Energy Technology Center under Contract No. DE-AC22-86PC90011, explored conversion of methane to useful products by two techniques that do not involve oxidative coupling. The first approach was direct catalytic dehydrocoupling of methane to give hydrocarbons and hydrogen. The second approach was oxidation of methane to methanol by using heterogenized versions of catalysts that were developed as homogeneous models of cytochrome-P450, an enzyme that actively hydroxylates hydrocarbons by using molecular oxygen.

Two possibilities exist for dehydrocoupling of methane to higher hydrocarbons: The first, oxidative coupling to ethane/ethylene and water, is the subject of intense current interest. Several researchers have recently pointed out that with oxidative coupling the apparent upper limit on yield of C_2 hydrocarbons is around 30% at atmospheric pressure. Nonoxidative coupling to higher hydrocarbons and hydrogen is endothermic, but in the absence of coke formation the theoretical thermodynamic equilibrium yield of hydrocarbons varies from 25% at 827°C to 65% at 1100°C (at atmospheric pressure). Additionally, the unreacted methane can readily be recycled after separation.

In this project we synthesized novel, highly dispersed metal catalysts by attaching metal clusters to inorganic supports. These catalysts were active in the conversion of methane to C_2 and higher hydrocarbons at 750°C in a fixed-bed, down-flow reactor under anaerobic conditions. Up to 50% selectivity for higher hydrocarbons was observed with alumina-supported hexameric ruthenium clusters. Zeolite-supported tetrameric clusters produced less coke than other catalysts tested, apparently because the cluster was located inside the zeolite supercage.

The second approach mimics microbial metabolism of methane to produce methanol. Applying biological catalysts to methane conversion provides a substantial energy-saving option because the reaction occurs at ambient temperature and pressure. However, the reaction rates are too slow and the methanol yields are generally too low for a commercial process. The methane mono-oxygenase enzyme responsible for the oxidation of methane to methanol in biological systems has exceptional selectivity and very good rates. The enzymatic activation of alkane C-H bonds is currently a very active area of research. Enzyme mimics are systems that function as the enzymes do but overcome the problems of slow rates and poor stability. Most of that effort has

focused on mimics of cytochrome P-450, which is a very active selective oxidation enzyme and has a metalloporphyrin at the active site. The interest in nonporphyrin mimics coincides with the interest in methane mono-oxygenase, whose active site has been identified as a μ-oxo dinuclear iron complex. In this project we employed mimics of cytochrome P-450, heterogenized to provide additional stability.

The oxidation of methane with molecular oxygen was investigated in a fixed-bed, down-flow reactor with various anchored metal phthalocyanines (PC) and porphyrins (TPP) as the catalysts. These supported organometallic species were stable at temperatures as high as 400°C. Methanol was formed in low yields from zeolite ecaged RuPC, CoTPP, and MnTPP at 375°C. In contrast, a PdPC complex attached to magnesia produced low yields of ethane rather than methanol. The other surface-supported catalysts gave only complete combustion products.

TABLE OF CONTENTS

FIGURES

TABLES

INTRODUCTION AND OBJECTIVES

The United States will need to be able to convert coal to liquid fuels should current supplies of liquid fuels be interrupted. Two indirect methods are available for producing fuel liquids: (1) gasification of coal to synthesis gas (syngas) followed by Fischer-Tropsch synthesis (FTS)[1] to convert syngas to hydrocarbons, and (2) a three-step process that includes gasification, conversion to methanol, and then conversion of methanol to hydrocarbons. Both processes are currently run commercially, the first in South Africa and the second in New Zealand. However, both the gasifier[2] and the FTS[3,4] processes result in the production of methane and/or light hydrocarbon by-products that increase the cost of producing liquid fuels from coal. The objective of the present research for the Department of Energy (DOE) was to develop catalysts that directly convert methane and light hydrocarbons to intermediates which later can be converted to either liquid fuels or value-added chemicals, as economics dictate.

We explored two approaches to developing such catalysts in this program. The first approach consists of developing advanced catalysts for dehydrocoupling methane. We prepared the catalysts by reacting organometallic complexes of transition metals (Fe and Ru) with zeolitic and rare-earth-exchanged zeolitic supports to produce surface-confined metal complexes in the zeolite pores. We then decomposed the organometallic complexes to obtain very stable, highly dispersed catalysts. The increased activity of highly dispersed catalysts is desirable for activating the relatively inert methane, and highly dispersed catalysts are more resistant to coking. The use of zeolitic supports will stabilize the highly dispersed catalysts, and the acidic nature of the zeolite is likely to contribute to the reforming chemistry.

Our second approach entailed synthesizing the porphyrin and phthalocyanine complexes of Cr, Mn, Ru, Fe, and/or Co within the pores of zeolitic supports for use as selective oxidation catalysts for methane and light hydrocarbons. Porphyrins and phthalocyanines are potent oxidants that also allow careful control of the active form of oxygen and thereby lead to control of activity and selectivity. The use of zeolitic supports enhances the stability and reactivity of the catalysts and discourages the secondary reactions that always pose problems in the oxidation of methane because the primary products are more easily oxidized than methane.

BACKGROUND

The primary difficulty with conversion of methane to more useful products is its inertness because of strong C-H bonds [BDE = 105.1 kcal/mol (BDE is bond dissociation energy)][5] and the absence of other mechanistic routes for derivatization. This is a kinetic problem. Other hydrocarbons, and particularly the desirable products of methane activation, have weaker C-H bonds and therefore react more quickly (for example, the C-H BDE of ethane is 98.2 kcal/mol). Methane is not particularly stable thermodynamically (ΔH_f°=-17.9 kcal/mol, compared with ΔH_f°=-20.2 kcal/mol for ethane,
ΔH_f°=-48 kcal/mol for methanol, and ΔH_f°=-94 kcal/mol for CO_2).[6] The three most promising approaches for conversion of methane are partial oxidation, oxyhydrochlorination, and dehydrocoupling. Partial oxidation has recently been reviewed by Pitchai and Klier[7] and by Gesser et al..[8] Oxyhydrochlorination processes have recently been developed.[9] This section briefly discusses the thermodynamic basis of the difficulty in controlling the activation reactions of methane and then briefly reviews previous attempts to improve product selectivity.

THERMODYNAMICS

The free energies of a number of reactions of potential use for derivatizing methane are listed in Table 1.[10] The most striking feature is that all the reactions involving oxidation are exothermic while all those involving dehydrogenation are endothermic, with the exception of formation of graphite at high temperatures. The oxidation is progressively more exothermic for continued oxidation, a feature that makes thermodynamic control of methane oxidation selectivity impossible.

OXIDATIVE COUPLING

The favorable energetics of oxidative coupling makes it a subject of intense current interest. Catalysts for this process have recently been reviewed by Lee and Oyami[11] and Hutchings et al.[12] However, as seen in Table 1, the oxidation is progressively more exothermic for continued oxidation, and this thermodynamic control of methane oxidation selectivity is impossible. Labinger[13] and others[14] recently pointed out that with oxidative coupling, the apparent upper limit

on the yield of C_2 hydrocarbons is about 30% at atmospheric pressure. Oxidative coupling also results in production of carbon oxides, which lower carbon yields and complicate the separation

Table 1

FREE ENERGY OF REACTIONS OF METHANE*

Reaction	Free Energy (kcal/mol of methane) $\Delta G_{427°C}$	ΔG_{1000K}
$2CH_4 \longrightarrow C_2H_6 + H_2$	8.5	8.5
$2CH_4 \longrightarrow C_2H_4 + 2H_2$	14	19.5
$2CH_4 \longrightarrow C_2H_2 + 3H_2$	25	16
$6CH_4 \longrightarrow C_6H_6 + 9H_2$	11	5.8
$CH_4 \longrightarrow C_{graphite} + 2H_2$	3.1	-4.6
$2CH_4 + H_2O_2 \longrightarrow C_2H_6 + H_2O$	-16	-14
$2CH_4 + O_2 \longrightarrow C_2H_4 + 2H_2O$	-36	-36
$2CH_4 + 3/2O_2 \longrightarrow C_2H_2 + 3H_2O$	-50	-53
$CH_4 + 3/2O_2 \longrightarrow CO + 2H_2O$	-138	-144
$CH_4 + 2O_2 \longrightarrow CO_2 + 2H_2O$	-191	-191
$CH_4 + O_2 \longrightarrow CO + H_2 + H_2O$	-88	-98
$CH_4 + 1/2O_2 \longrightarrow CO + 2H_2$	-38	-53
$CH_4 + 1/2O_2 \longrightarrow CH_3OH$	-22	-18

*Source: Ref. 10.

and recycle processes. Two recent articles report on processes that circumvent the carbon oxide part of the problem with oxidative coupling. First, Heinemann and coworkers reported on a low temperature oxidative coupling process[15] (< 600°C), using low oxygen/methane ratios and steam, which results in very low production of carbon oxides. Second, workers at Institut Francais du

Petrole (IFP)[16] reported on injecting ethane into the process stream after a short contact with the methane/oxygen mixture to consume all the oxygen. In this process the ethane is cracked, giving ethylene and hydrogen, which can react with the carbon oxides to form methane and water. The result is very low net carbon oxide yields and enhanced net ethylene yields.

An intriguing recent publication reports achieving 50% yield of C_2 products (65% conversion with 80% selectivity).[17] Samarium oxide was used as catalyst in a reactor designed to simulate a countercurrent moving-bed chromatographic reactor. The improvement is primarily due to the rapid separation of O_2, CH_4, and the C_2 products that occurs in this reactor.

DEHYDROCOUPLING

Thermal dehydrocoupling producing higher hydrocarbons and hydrogen (pyrolysis) is endothermic, but in the absence of coke formation, the theoretical thermodynamic equilibrium yield of hydrocarbons varies between 25% at 827°C and 65% at 1100°C (at atmospheric pressure).[18] Additionally, the unreacted methane can easily be separated and recycled. These yields are very attractive, and recent reports (summarized in Table 2) appear to confirm this concept.[19-28] The results reported by Yamaguchi et al.,[23] IFP (Mimoun et al.[16]), and Chevron (Devries and Ryason[26]) all appear very promising, with conversions ranging from 30% to 50% and hydrocarbon selectivities ranging from 75% to 100%. These results are very close to the thermodynamic equilibrium values. The major product in most of these studies is aromatic hydrocarbons.

Early indications that dehydrocoupling of methane is feasible come from chemisorption studies of methane on metals. Methane is readily activated by metals in a dissociative chemisorption process to give hydrogen. Table 3 lists a collection of the temperatures of dissociative chemisorption of methane on a number of metals.[29] These values were determined by measuring the appearance of hydrogen in the gas mixture above these metals in the presence of methane.

Ceyer and coworkers[30] have reported 100% gas phase selectivity for benzene production from methane over Ni at low temperatures under high vacuum conditions. This high selectivity is achieved by physisorbing methane at low temperature on the nickel surface. The adsorbed methane is then dissociated and gives chemisorbed methane by colliding with energetic inert gas atoms. The chemisorbed methane is then heated to allowing coupling first to adsorbed acetylene and then to benzene, which desorbs. In these experiments, the hydrogen desorbed at about 130°C and the benzene at 145°C.

Table 2

LITERATURE REPORTS ON THERMAL DEHYDROCOUPLING OF METHANE

Catalyst	Reference	Temp. (°C)	Conversion (%)	C_2 Select. (%)	C_{3-5} Select. (%)	C_6^+ Select. (%)
$CaCrPt/Al_2O_3$	19	705	28	31	?	68
GeO_2/SiO_2	20	700	0.2	51	?	3.3
Ge zeolite	21	700	3.8	?	?	51
Ge thoria	22	>1000	25	30	?	60
W	23	1300	50	?	?	85
Ru/Al_2O_3	24	750	6	7	?	41
Ru/MgO	24	750	4	7	?	49
Ru/MgO	25	1200	31	55	?	23
BN	26	1130	35	36	?	64
Zeolites	27	600	?	?	?	6.4
Euro Pt-1	28	250	19	63.5	34	2.5

Table 3

TEMPERATURES OF DISSOCIATIVE CHEMISORPTION*

Metal	T_{H_2}(°C)
Re	20
Rh	50
Mo	80
Ni	100
Pd	125
Ta	225
Ti	320

*Source: Ref. 30.

Amariglio and coworkers reported[31] on conversion of methane to C_2 and higher hydrocarbons over platinum at 250°C. They used a pulse sequence in which methane was first adsorbed for 1 min followed by a hydrogen purge to remove the carbonaceous residue from the catalyst surface. They estimated that 19% of the methane was converted to higher hydrocarbons. They calculated that they had achieved about 40% of the equilibrium conversion of methane to ethane and hydrogen. The selectivities observed were 63.5% selectivity to C_2 products, 13% to C_3, 8% to C_4, 13% to C_5, and only 2.4% to C_6 products.

Cserenyi's group[32] subsequently studied the platinum group metals. Their conditions were slightly different: 250°C and a flow of 12.5% CH_4 in N_2. They observed formation of hydrogen and ethylene in the early stages of the experiment, but the rate of formation of these products fell off rapidly over a 20-min period. The most active catalyst for H_2 production was Rh, and the most active for ethane production was Pt. They calculated that over Pt they achieved about 40% of the equilibrium conversion of methane to ethylene and hydrogen. Reaction with hydrogen after the exposure to methane permitted recovery of additional hydrocarbons and return of the catalyst to its original activity.

Van Santen and coworkers[33] developed a similar process where the methane is adsorbed at around 450°C and the hydrocarbons are removed from the surface by hydrogenation at around 100°C. They studied a wide variety of potential transition metal catalysts and found the best yields (13%) over ruthenium catalysts.

OXIDATION TO METHANOL

Partial oxidations of methane to methanol and formaldehyde over homogeneous and heterogeneous catalysts have been demonstrated.[7] However, nitrous oxide, commonly used as the oxidant, is expensive compared with air or oxygen. In addition, the moderately high reaction temperature (400-500°C) also leads to oxidation of the desired products, methanol and formaldehyde, to carbon oxides. Chun and Anthony[34] studied the conventionally catalyzed oxidation of methane to methanol and found that with 10:1 ratios of methane to oxygen and high oxygen conversions the selectivity to methanol is between 30% and 35% at reasonable pressures. These selectivities were independent of catalyst, apparently because the reactions were dominated by homogeneous reactions and the role of the catalyst was to shorten the chain length and thus minimize overoxidation.

Recent attention has focused on the electrophilic oxidation of methane to give methanol.[35-37] The reaction is shown schematically in Scheme 1.

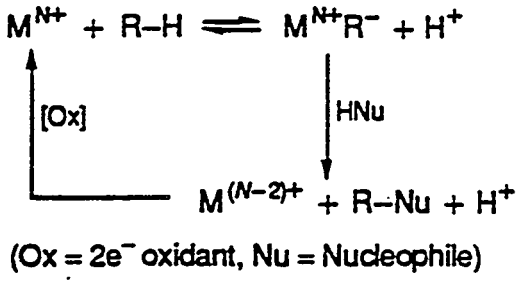

Scheme I: Electrophilic Oxidation of Methane

The key step is the cleavage of a C-H bond by an electrophilic metal such as Pt(II), Pd(II), or Co(III). These reactions are characterized by relatively low yields. A recent publication describes a related approach in which much higher yields are achieved using Hg(II) [or Th(III), Pt(II), Pd(II), or Au(II)] in sulfuric acid as the oxidant.[38] The system was reported to give 85% selectivity with mercury turnovers of 4 per hour at 180°C [versus 0.2 turnovers per hour for the Pd(II) case discussed above[36]]. A similar electrophilic mechanism was proposed for this process. However, the mechanism of this reaction has been challenged; the alternative mechanism proposed is that this reaction involves a series of electron transfers and the intermediacy of radicals and carbocations.[39]

Applying biological catalysts to methane conversion provides a substantial energy-saving option because the reaction occurs at ambient temperature and pressure. Organisms that are able to convert methane to methanol have been discovered,[40,41] but the reaction rates are too slow and the methanol yields are generally less than 1%. Three major problems to be overcome are the mass transfer rate of gas phase methane to the aqueous phase; the cell density, which limits the catalyst concentration; and the system design for isolation of products. Also, the bacteria usually metabolize methane completely to CO_2, with methanol as an intercellular intermediate. Therefore, methanol production using biological catalysts requires manipulation of the enzymatic reactions by regulating the electron transport and environmental conditions to favor the methane mono-oxygenase pathway, which gives the methanol extracellularly.[41]

The enzymatic activation of alkane C-H bonds is currently an important area of research. Metal complexes that mimic the active site of enzymes have been synthesized and investigated under homogeneous conditions. Considerable effort has been focused on mimics of cytochrome P-450, which has a metalloporphyrin center at the active site.[42-44] The interest in nonporphyrin complexes as C-H activation catalysts coincides with the interest in methane mono-oxygenase,

which has been shown to have a μ-oxo dinuclear iron complex.[45,46] Enzyme mimics are being developed to overcome the enzyme systems problems of poor rate and limited lifetimes.

Mono-oxygenase Mimics

Transition metal complexes have been synthesized as models for the mono-oxygenases.[47-49] Many of these models have been metalloporphyrins, since an iron-containing heme is the prosthetic group in cytochrome P-450, a remarkable enzyme that can hydroxylate any organic substrates, including alkanes.[50] The central metal in these synthetic models is most often iron or manganese, but chromium, cobalt, copper, vanadium, and ruthenium have also been investigated. These systems are most often used with an oxygen atom donor such as iodosobenzene, hypochlorite, or peroxide. These metalloporphyrins have been shown to oxidize alkanes to alcohols, epoxidize olefins, produce methyl ketones from terminal olefins, and dealkylate anisole, all of which are reactions catalyzed by mono-oxygenase.[50,51] Porphyrins with manganese as the central metal can use oxygen itself as the oxygen atom source in the presence of reducing agents such as ascorbate or zinc[52]; the need for reduction of the metal before activation of oxygen is very similar to the case in the mono-oxygenase process.

Several nonporphyrin iron-based systems have also been studied as models for mono-oxygenase. For example, iron(II) EDTA was used to hydroxylate substituted benzene in the presence of ascorbic acid and oxygen.[53] The ascorbate can be replaced by many other reductants.[54] Iron(III) catechol and hydrogen peroxide can also hydroxylate the benzene ring.[55] A mixed valence tri-iron cluster was able to oxidize hydrocarbons in a nonradical pathway, although the overall yields were poor.[56] Ono and Katsube compared several iron-based systems in the oxidation of bencyclane.[57] Aliphatic hydroxylation was observed with simple systems or when cyclodextrin was added; with other organic ligands added, such as phenol, catechol, or tetraphenylporphyrin, aromatic hydroxylation was preferred. This selectivity was attributed to differences in control of the substrate binding when the coordinated ligand was varied.

Copper-based systems have also been examined as mimics of mono-oxygenase. Karlin and coworkers[58] worked with polypyridyl complexes of Cu(I), which hydroxylate the central aromatic ring in the presence of oxygen. Merrill and coworkers [59] synthesized mononuclear complexes of copper that can react with oxygen reversibly; however, the reactivity with substrates was not examined. Cu(II) with peroxide reacts with phenols to give catechols.[60]

Several complexes with nonbiomimetic metal ions have recently been investigated as models for the reactivity of mono-oxygenase. Daire and coworkers[61] show that a peroxo-

chromium complex oxidizes aliphatic hydrocarbons to alcohols and ketones. A nickel complex that binds oxygen reversibly in water has been used to hydroxylate aromatic species to phenol but not to catechols.[62] A recently reported cobalt complex with a nonporphyrin ligand expoxidizes styrene.[63] Srinivasan and coworkers demonstrated that manganese Schiff-base complexes can epoxidize olefins and hydroxylate hydrocarbons; electron-withdrawing substituents on the benzene ring enhanced the reactivity of the complex.[64]

Recent reports on methane mono-oxygenase showed that the enzyme contained a μ-oxo di-iron nonporphyrin active site.[65,66] Fish and coworkers[46,67] recently used iron and manganese clusters to hydroxylate C_2, C_3, and cyclo-C_6 hydrocarbons in the presence of *t*-butyl hydroperoxide. An important factor for small hydrocarbon activation might be the shape selectivity of the catalyst. Changing the ligand environment could provide the shape selectivity to trap methane and provide the kinetic advantage for C-H activation. Using a computer-aided molecular design technique, Shelnutt and coworkers[68] synthesized porphyrins that contained bulky carborane groups to mimic the hydrophobic pocket of cytochrome P-450. The cavity was designed to control the access of various substrates, oxidants, products, and solvents to the reactive metal center. Another approach to control the cavity in which the oxidation occurs is to confine the active catalyst inside zeolite cages.[69]

APPROACH

SRI's development of improved catalytic processes for the direct conversion of methane and light hydrocarbon gases to olefins or alcohols consisted of four tasks that represent two distinctly different approaches to the problem. In Tasks 1 and 2, we sought to develop advanced dehydrocoupling catalysts for use in the production of olefins or aromatics. These catalysts consisted of highly dispersed, very stable metal particles that are produced by the decomposition of surface-confined metal clusters of controlled size, shape, and composition. In Tasks 3 and 4, we sought to develop oxidation catalysts of high activity that selectively produce alcohols. We prepared catalysts by synthesizing known homogeneous oxidation catalysts in the pores of zeolite supports. The four tasks are described in more detail below and in the next section.

TASK 1: SYNTHESIS OF ADVANCED DEHYDROCOUPLING CATALYSTS FOR METHANE

We synthesized methane dehydrocoupling catalysts in Task 1 by thermally decomposing surface-confined metal clusters of carefully controlled size. The variables we studied included cluster size, cluster composition, and activation procedures. The support materials we investigated included alumnia, zeolites, and rare-earth-exchanged zeolites; the metal complexes studied were the carbonyl clusters of Fe and Ru and their mixtures. Clusters of two to four metal atoms were used as catalyst precursors.

Research is under way on the techniques of surface confinement to produce novel catalysts for a wide variety of processes, [70-90] e.g., SRI's studies of the techniques for HDN catalysis (DOE Contract No. DE-FG22-85P8C80906) and of FTS catalysis (DOE Contract No. DE-AG22-85PC80016). The stability of surface-confined clusters prepared by reaction of multinuclear carbonyl complexes with the surface of oxide supports in an ill-defined reaction has been questioned.[91] Therefore, to prepare catalysts whose surface binding is better characterized, we studied catalysts of the Yermakov type, which are anchored by direct reaction with the surface [Reaction (1)].

$$RM_xL_n + HO\text{–(surface)} \longrightarrow RH + L_nM_x\text{–O–(surface)} \qquad (1)$$

Where R is alkyl, M is metal, and L is other support ligand such as carbonyl. Alkyl metal complexes are known for all the metals in question.[92]

Specifically, we generated surface-confined metal complexes by using Reaction (1): Alkyl metal complexes for use in Reaction (1) were prepared from the hydridocarbonyl clusters by the reaction of triethyl aluminum [Reaction (2)] and the surface-confined clusters generated by Reaction (3).

$$H_2Ru_3(CO)_{11} + AlEt_3 \longrightarrow EtH + Et_2Al(H)Ru_3(CO)_{11} \quad (2)$$

$$Et_2AlRu_3(CO)_{11} + HO\text{–(surface)} \longrightarrow EtH + H(CO)_{11}Ru_3(Et)Al\text{–O–(surface)} \quad (3)$$

The carbonyl clusters used for reaction with the triethyl aluminum included $H_2Ru_3(CO)_{11}$, $H_2Ru_4(CO)_{13}$, and $H_2Ru_6(CO)_{18}$ for Ru, and the mixed Fe/Ru cluster, $H_4Ru_3Fe(CO)_{13}$.

TASK 2: TESTING OF METHANE DEHYDROCOUPLING CATALYSTS

The majority of the testing was conducted in a fixed-bed isothermal microreactor in a down-flow mode at moderate pressure. An automated Carle two-column gas chromatograph (GC) was used to monitor the conversion of methane and product formation. Variables included space velocity and temperature. A commercially available ruthenium-on-alumnia catalyst was used as the baseline.

A small number of tests were conducted in a reactor equipped with a stabilized Pd membrane *in situ* to control the H_2 partial pressure.[93] Variables studied included space velocity of methane, temperature, and sweep gas or vacuum. We first designed a reactor with a sweep gas flowing on the permeate side of the membrane reactor as shown in Figure 1.

This reactor configuration caused difficulties because of the seals between the Pd/Ag tube of the membrane and the stainless steel (SS) reactor. A modified design, shown in Figure 2, solved this problem by reducing the number of seals to one and removing the seal from the hot zone. However, this design did allow for a flow of sweep gas on the permeate side.

TASK 3: SYNTHESIS OF OXIDATION CATALYSTS FOR METHANE

We synthesized oxidation catalysts by encapsulating porphyrin and phthalocyanine metal complexes in zeolites. Variables studied included the porphyrin or phthalocyanine ligand, the type

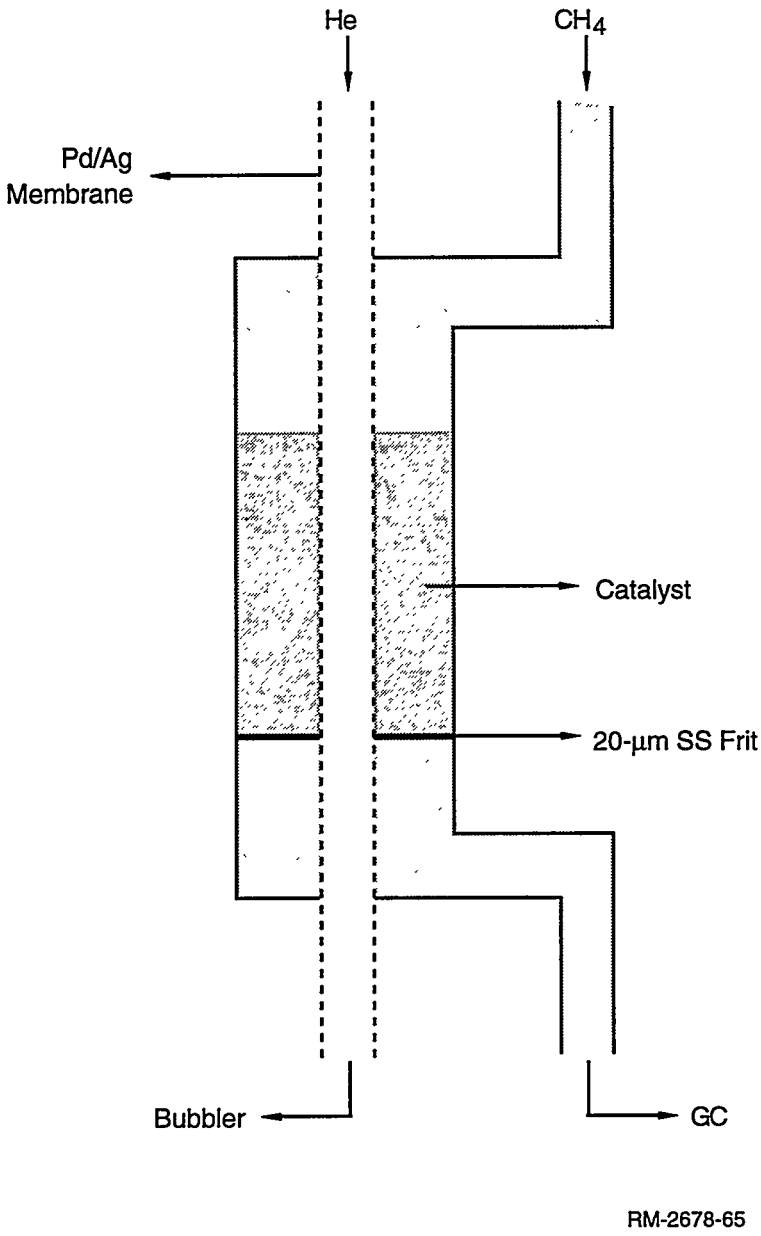

Figure 1. Reactor equipped with Pd/Ag membrane.

SS = stainless steel.

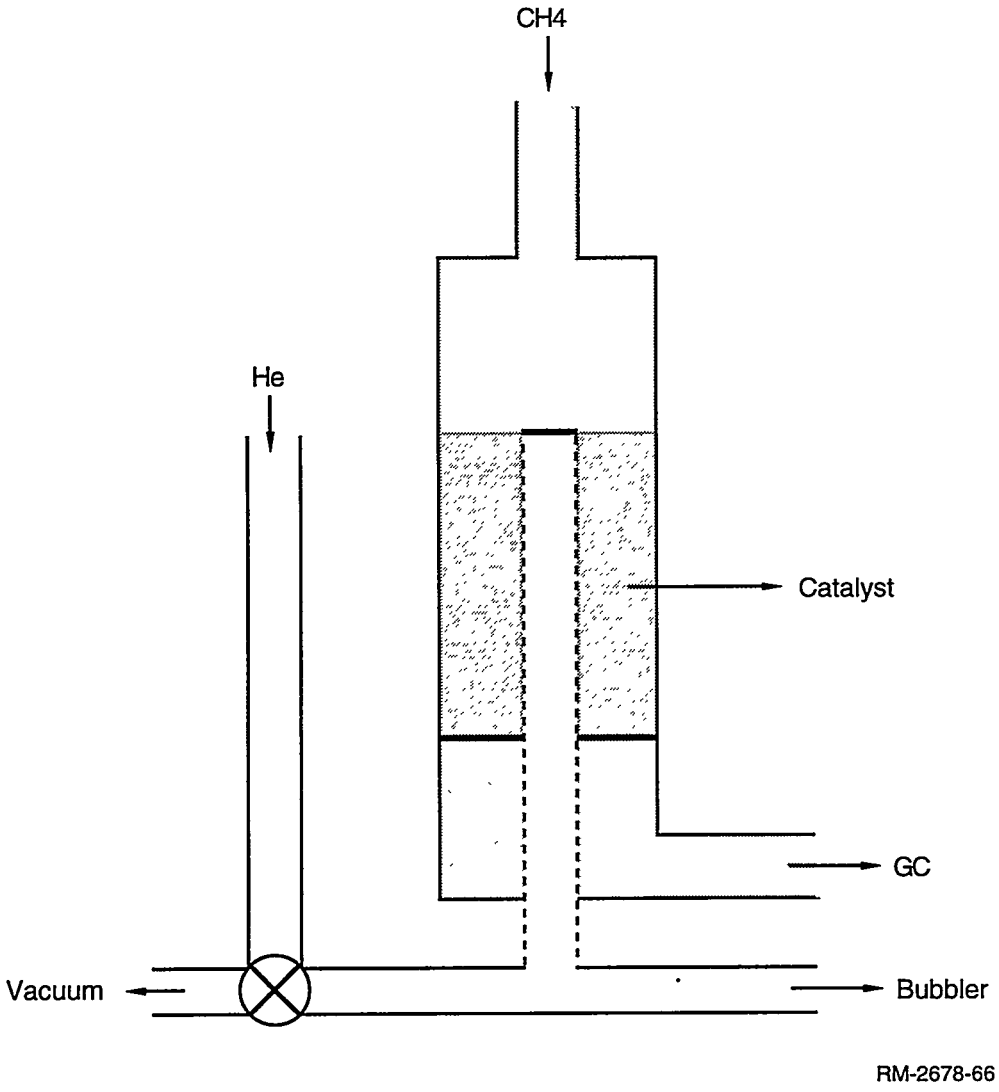

Figure 2. Modified reactor equipped with Pd/Ag membrane tube.

of metal, and the type of zeolite. The types of metal studied included Ru, Mn, Fe, Pd, Cu, Mo, and Co, with emphasis on the Ru examples.

The porphyrin and phthalocyanine complexes were synthesized within the zeolite pore by first exchanging the metal ion into the pore and then condensing the template.[94] For porphyrins, the condensation of appropriately substituted pyrroles [Equation (4)] gave the desired porphyrin.

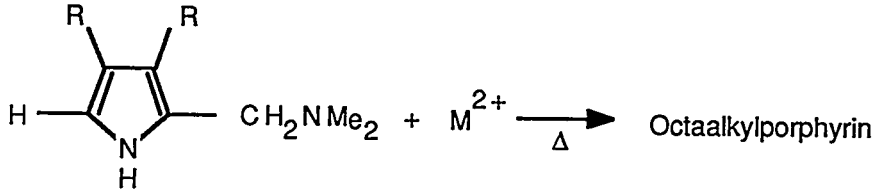

(4)

Alternatively, the co-condensation of pyrrole with benzaldehyde gave tetraphenylporphyrin [Equation (5)].[95]

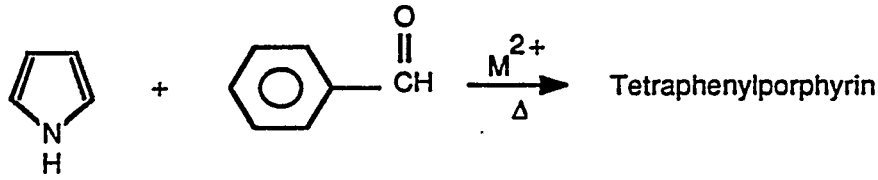

(5)

The phthalocyanines were produced by the condensation of phthalonitriles [Equation (6)].

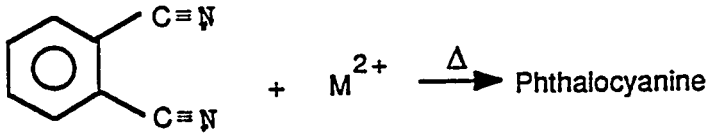

(6)

Alternatively, condensation of phthalic anhydride and urea produced phthalocyanine [Equation (7)][96]

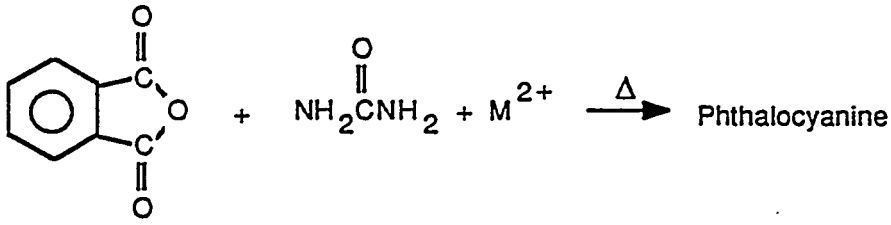

(7)

TASK 4: TESTING OF METHANE OXIDATION CATALYSTS

We tested methane oxidation catalysts in the same fixed-bed isothermal down-flow reactor used in Task 2. We used an automated two-column GC to monitor the conversion of methane and oxygen and product formation. Low oxygen concentrations were used initially. Variables included space velocity, temperature, and feed composition. For comparative purposes, a commercially available oxidation catalyst (vanadium pentoxide, manufactured by American Cyanamid) was also used.

EXPERIMENTAL

GENERAL METHODS

The reactions were conducted in the fixed-bed isothermal microreactor described above.[97-99] The exhaust gases from the reactor passed through a trap for liquid removal and then through a sampling valve for periodic sampling by an automated two-column Carle GC. The liquids recovered from the liquid trap were analyzed by a second GC (HP5890) or a HP1090 high-pressure liquid chromatograph (HPLC).

The chemical natures of the catalysts were determined by spectroscopic techniques. Basset and Choplin have shown that UV-VIS spectroscopy can be used to characterize surface-confined catalysts.[81] The technique is particularly good for the porphyrin and phthalocyanine catalysts because their characteristic UV-VIS bands are quite strong. IR spectra were measured and compared with data from literature studies of surface-confined clusters.[100-104]

TASK 1: SYNTHESIS OF METHANE DEHYDROCOUPLING CATALYSTS

Synthesis of Ruthenium Compounds

$H_4Ru_4(CO)_{12}$,[105] $H_2Ru_6(CO)_{18}$,[106] $H_2FeRu_3(CO)_{13}$,[107] $Ru(C_3H_5)_2(CO)_2$,[108] and $NaRu(C_3H_5)(CO)_3$[108] were prepared by literature methods with strict exclusion of air and stored in a dry-box until needed. It is critical to use anhydrous acid in acidifying the hexaruthenium cluster to give the dihydride, since the presence of water leads to incomplete protonation of the cluster. A typical synthesis of one of the clusters is described below. Preparation of $H_4Ru_4(CO)_{12}$ and $H_2Ru_6(CO)_{18}$ is discussed under Task 1 in the Results and Discussion section.

Preparation of $H_2FeRu_3(CO)_{13}$

A tetrahydrofuran (THF) (120 mL) solution of $Ru_3(CO)_{12}$ (300 mg, Aldrich) was added dropwise over 30 min to a refluxing THF (250 mL) solution of $Na_2[Fe(CO)_4]$ (210 mg, Aldrich) and the solution was allowed to reflux for 1 h. The solvent was immediately removed from the deep red solution under vacuum. Then 120 mL of deoxygenated hexane was added to the brown residue, followed by 40 mL of deoxygenated H_3PO_4. The hexane layer was separated, dried over

anhydrous $MgSO_4$ for 1 h, and then filtered. The brown solution was concentrated to 60 mL and chromatographed on silica gel. Hexane was used as eluent to remove $Ru_3(CO)_{12}$, $H_4Ru_4(CO)_{12}$, and $Fe_3(CO)_{12}$. A solution of 10% acetone in hexane was used to elute the red $H_2FeRu_3(CO)_{13}$. The product was recrystallized in hexane (yield 40 mg, 11.7%). The IR spectra agreed with the literature.

Preparation of Aluminum-Ruthenium Clusters

The same procedure was typically used for all preparations. The technique used here, attaching hydrido ruthenium clusters to acidic supports by first reacting them with triethylaluminum, was first developed by SRI on a previous DOE project (Contract DE-AG22-85PC80016).[97] The ruthenium clusters prepared as described above were redissolved in hexane and placed in a vacuum flask attached to a vacuum line equipped to measure the gas generation. One equivalent of triethyl aluminum was added to the solution, and the evolved ethylene was collected until gas evolution ceased. The evolved gas was checked by GC and found to contain only ethylene. In all cases, the measured ethylene was equivalent to one ethylene evolved per metal cluster. The product was characterized by IR and nuclear magnetic resonance (NMR) spectroscopy.

Preparation of Supported Ruthenium Clusters on Acidic Supports

Each of the metal clusters was supported on alumnia, 5-Å molecular sieves, and LZ-Y52 Y-zeolite by using the same procedure: The support was dried for 10 h at 500°C under vacuum. The Bronsted acid site density of each support was measured by titration with ethyl lithium and the quantity of cluster added adjusted to maintain an excess of surface hydroxyl groups. The dried support was placed in a vacuum flask and THF solvent added. The flask was then attached to the vacuum line equipped to measure gas generation. A THF solution of the triethylaluminum modified ruthenium cluster was added to this slurry and the ethylene collected. No carbon monoxide was detected. In each case, 1 eq. of ethylene evolved per metal cluster. The solution went colorless, an indication that all the ruthenium cluster reacted with the surface.

Preparation of Supported Ruthenium Monomer on Acidic Supports

Monomeric ruthenium catalysts were prepared on alumnia, 5-Å molecular sieves, and LZ-Y52 Y-zeolite by reacting $(allyl)_2Ru(CO)_2$ with the support in THF at 25°C. No gas evolution was detected, but the solution went colorless, an indication of complete reaction with the support.

Preparation of Magnesium Oxide Supported Clusters.

Magnesium oxide supported clusters were prepared as follows: the acidic clusters—ruthenium hydride clusters such as $H_4Ru_4(CO)_{12}$, $H_2Ru_6(CO)_{18}$, and $H_2FeRu_3(CO)_{13}$—were dissolved and added to magnesium oxide that had been previously dried at 500°C for 6 h. The mixture was stirred overnight, during which time the solution went colorless, an indication that all the cluster had adsorbed. The solid was then filtered and dried.

Preparation of Magnesium Oxide Supported Ruthenium Monomer (RuMgO)

To a solution of $Na(C_3H_5)Ru(CO)_3$ (124mg) in THF (30 mL) was added 5 g of magnesium oxide that had been previously dried at 500°C for 6 h. After the mixture was stirred for 16 h, the solvent was removed under reduced pressure at ambient temperature. The catalyst was activated at 200°C under helium flow before methane was introduced. Elemental analysis for ruthenium showed 0.20%.

TASK 2: TESTING OF METHANE DEHYDROCOUPLING CATALYSTS

A schematic representation of the reactor system is shown in Figure 3. The system has five gas inlet ports: one each for methane and oxygen, one for helium purge, one for hydrogen (which can be used to reduce the catalyst), and one spare inlet port for a reaction initiator such as ethane. The gases are filtered through a 1-μm in-line filter, after which they pass through a vented inlet system controlled by a three-way valve. This inlet arrangement allows for changes in the feed gas composition without having to shut down the reactor system.

The gas flows are controlled by mass flow controllers (Brooks 5800 series). Check valves are installed after the mass flow controllers to prevent back flow. The pressure of the gas mixture is indicated by a pressure gauge and a pressure transducer. An adjustable pressure relief valve is connected to the reactor effluent line. A vacuum line is also connected for activating the catalyst and for removing air in the system after a change of catalyst. The reactor is equipped with quick connects on both ends to allow rapid change of catalyst without exposure to air and a thrmocouple immersed in the catalyst bed for temperature control. The outlet gas from the reactor is led through a back pressure regulator, a pressure gauge, and a needle control valve that is used to control the flow rate. The gas is then introduced to the gas sampling valves inside the Carle 500 GC and then vented through an oil bubbler and a soap-film flowmeter. The bubbler prevents any back diffusion of air and serves as a flow indicator.

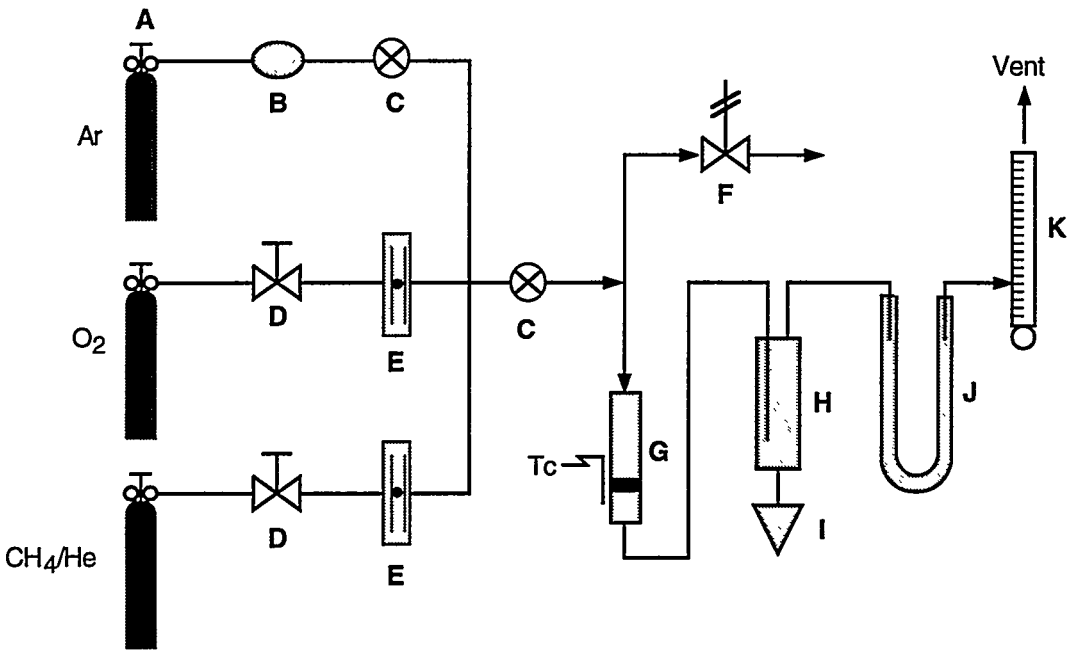

A. Pressure regulator
B. Purifier (gas and ring tube)
C. Manually operated valve
D. Needle control valve
E. Flow meter
F. Pressure relief valve, cracks at indicated pressure (50 psi)
G. Reactor
H. Condenser
I. Liquid collector
J. Bubbler
K. Soap-film slow meter

RM-2678-43

Figure 3. Isothermal reaction unit.

The maximum operating pressure of this system is 250 psi, which is limited by the quick connects and the back pressure regulator. A higher pressure limit can be achieved by simple replacement of these components if desired at a later stage of the development.

General Procedure for Testing Methane Dehydrocoupling Catalyst

The catalyst (500 mg) is loaded into the ss reactor (0.22-in. internal diameter) in the dry-box. The reactor is connected to the reactor system and purged with helium for 15 min. A helium diluted methane gas (containing about 20% methane) is passed through a mass flow controller to the reactor. The back pressure regulator is set at the desired pressure and the methane flow rate is controlled by the mass flow controller. A thermocouple is immersed in the catalyst bed and connected to a temperature controller, which controls the furnace. The outlet gases are fed to a Carle 500 GC for sample analysis. The GC is programmed to separate light gases including hydrogen, carbon oxides, air, and hydrocarbons up to C_5. The C_6 or higher hydrocarbons and other polar compounds (C_{6+}) are back flushed from the column to the detector. The calibration of the C_{6+} peak is based on the area integration and referenced to the methane peak. Other components are calibrated using a standard sample mixture at room temperature and calibrating the detector response to each component. Initial methane concentration is measured before and after each run at ambient temperature under the same pressure and flow rate.

We were concerned about the method of calibration of the GC. We checked by running another series of calibrations using a standard mixture of gases at three temperatures: room temperature, 550°C, and 750°C. The mixture contained C_1-C_4 saturated hydrocarbons, ethylene, hydrogen, carbon monoxide, carbon dioxide, oxygen, and nitrogen. This mixture was used to establish the relative response factors of these gases with respect to nitrogen, and how temperature affects these response factors in the empty reactor. Nitrogen is assumed to be inert under the reaction conditions, so that the volume percent (vol%) of nitrogen remains constant under all conditions. Use of nitrogen as an internal standard enables us to minimize the effects of variations in sample volume on the measurement of our reaction products as the temperature is changed. We assume that the number of moles of gas exiting the reactor is equivalent to the number entering. At low conversions of methane, this assumption is justified because the change is small compared to the total number of moles of gas. Methane is about 20 vol% of the entering gas mixture. Even if 5 vol% of the methane reacts to give no gaseous products (an unlikely event), the number of moles of gas leaving will have changed only 1%, which is within the error limits of the GC.

When we raised the temperature of the empty reactor, we observed several major changes in our standard mixture. At 550°C, all of the hydrocarbons remained constant with the exception of ethylene, which declines slightly. This decrease may be due to the presence of oxygen in the standard gas mixture used. At 750°C, we observed cracking of the hydro-carbons. Several new peaks were observed in the chromatogram, which were attributed to the appearance of propylene and butenes. The total C_2-C_4 saturated hydrocarbons declined drastically while the amount of methane and hydrogen rose. These blanks demonstrate that the reactor can catalyze further reactions of the primary hydrocarbon products at high temperatures, so we cannot determine the relative response factors of all the components to nitrogen at elevated temperatures. It also suggests that the conversions and selectivities we report are lower limits for the actual values, since the reactor can catalyze the back reaction of potential products such as propane and hydrogen to give methane. The area of the nitrogen peak in these injections remained constant, which is a good indication that the size of our injection volume is constant.

A gas mixture of 20.8 vol% methane and 20.5 vol% nitrogen (balance helium) was tested in the empty reactor at typical reaction conditions. By using the response factors calculated above at room temperature, the amount of methane was determined to be 20.85% at 550°C and 20.69% at 750°C. This variation is less than 1% and well within the experimental error of the GC (2%, according to the vendor), so the use of room temperature response factors at higher temperatures does not introduce greater error into our calculations.

The result of these calibration/blank experiments was to give us confidence that our data are reliable. We also ran some of the later experiments using nitrogen as an internal standard to check on reliability.

In-Situ Diffuse Reflectance FTIR Studies of the Catalysts

We used *in situ* Fourier transform infrared (FTIR) spectroscopy as a method to examine the mechanism of methane conversion over these supported metal clusters. We used a diffuse reflectance method using the sample holder shown in Figure 4. The sample holder fits into a pressure chamber equipped with IR windows that are capable of withstanding pressures of several hundred psi and are water cooled. The reactive gas is introduced into this pressure chamber and flows out through the sample as shown. The sample is heated and the temperature controlled using a thermocouple embedded in the sample. The sample must not be strongly absorbing in the IR region. This diffuse reflectance FTIR (DRIFTS) technique is very similar to the one recently

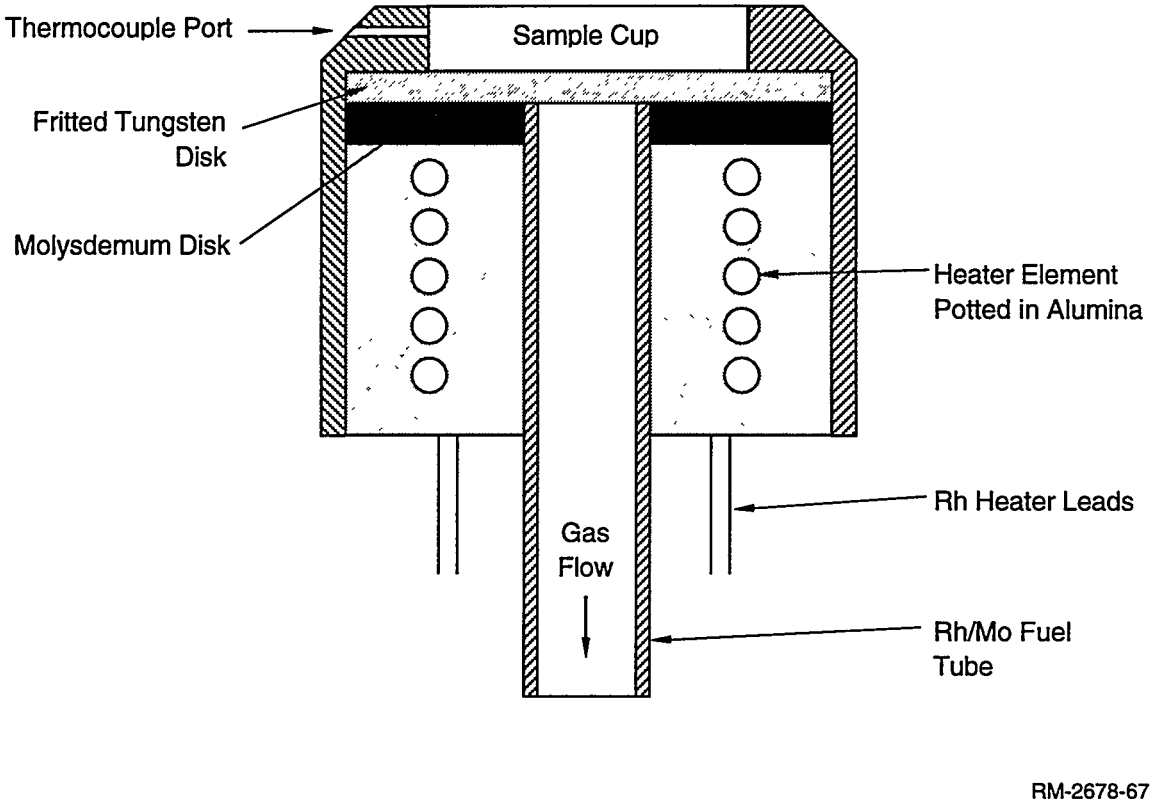

Figure 4. Sample holder for *in situ* diffuse reflectance FTIR studies of supported catalysts for methane conversion.

reported by Vannice.[109] We have been able to collect data using this system up to 600°C. We are unable to collect good spectra at 700°C.

TASK 3: SYNTHESIS OF METHANE PARTIAL OXIDATION CATALYSTS

Preparation of Metal Ion Exchanged Zeolite

To a slurry of 500 g zeolite (LZ-Y52, Union Carbide) and water (500 mL), 500 mL of a 1 M aqueous solution of metal salt ($FeCl_2$, $CoCl_2$, $MnSO_4$, or $Ru(DMSO)_4Cl_2$) was added dropwise over approximately 1 h. (In one case, a solution of $Ru_3(CO)_{12}$ in methanol was used.) The zeolite slurry was stirred at a constant speed. After the mixture was allowed to stir for 24 h, the exchanged powder was filtered, washed with water until the washing was free of chloride or sulfate, and then dried at 150°C under vacuum for 48 h. Elemental analysis results were as follows: Co-zeolite: C, 0.27; H, 0.91; Co, 4.76°. Fe-zeolite: C, 0.26; H, 1.20; Fe, 4.89°. Ru-zeolite: C, 1.16; H, 1.08, Ru, 0.95.

Preparation of Zeolite Encapsulated Metallophthalocyanine

(1) Metal exchanged zeolite (100g) and 8 eq. of 1,2-dicyanobenzene were added to 200 mL of nitrobenzene in a round-bottom flask fitted with a reflux condenser and a mechanical stirrer. The mixture was heated to 180°C for 4 h under nitrogen until the solution changed color (dark green for Fe, dark blue for Co, brown for Mn and Ru). The zeolite was filtered, washed with methanol to remove nitrobenzene, and Soxhlet extracted with pyridine until the solution was clear. Excess pyridine was removed by Soxhlet extraction with methanol. The zeolite powder was then boiled in a 1 M solution of NaCl (reverse metal exchange) for 4 h, then washed with water and acetone. Product was dried at 150°C under vacuum for 24 h.

(2) A mixture of 10 g of phthalonitrile (Aldrich) and 20 g of transition metal containing zeolite was ground to powder and added to a 100-mL round-bottom flask equipped with a reflux condenser. The mixture was heated to 250°C for 6 h. The formation of phthalocyanine was indicated by a color change to green. The green powder was allowed to cool to ambient temperature and then washed three times with excess methanol until the liquid was clear. The resulting product was then sublimed at 150°C under vacuum (1 mm Hg) for 2 h.

Preparation of Zeolite Encapsulated Tetraphenylporphyrin

Zeolite powder (200g) was added to 1.8L of acetic acid in a 2-L round-bottom flask equipped with a mechanical stirrer and an addition funnel that contained 46.5 mL pyrrole and 66.5 mL benzaldehyde. The acetic acid was heated to a boil. The pyrrole and benzaldehyde were added slowly. The reaction mixture was boiled for 0.5 h under air. The dark purple solid was filtered while the solution was still warm, then washed with a large amount of acetone until the washing was colorless. The product was dried at 150°C under vacuum for 24 h.

Metal Insertion of TPP in Zeolite

A mixture of TPP-zeolite (50 g) and metal salt [0.12 mol of $CoCl_2$, $FeCl_2$, $MnSO_4$, or $Ru_3(CO)_{12}$] was added to 200 mL of dimethyl sulfoxide (DMSO) in a three necked round-bottom flask equipped with a mechanical stirrer, a reflux condenser, and a gas inlet adapter. The reaction mixture was heated to reflux for 3 h. The product was washed with water and methanol. Excess metal salt was removed by boiling in a 1 M aqueous solution of NaCl for 2 h. The product was washed again with water and methanol and then dried at 150°C for 24 h.

Preparation of Zeolite Encapsulated Tetramesitylporphyrins ($TMPH_2$)

A mixture of Zn-Y zeolite (10 g, prepared by metal ion exchange method using $ZnCl_2$; metal weight loading estimated to be about 2%), mesitylaldehyde (3.6 g), pyrrole (1.6 g), and pyridine (0.5 mL) was added into a quartz tube placed inside a Parr bomb. The mixture was flushed with oxygen and sealed. The Parr bomb was heated at 180°C for two days. The brown zeolite was then removed and washed with a large amount of acetone.

The resulting zeolite was stirred in 6 N HCl for 2 h to remove zinc and then washed with water and 2 N NH_4OH. The zeolite was then washed again with water and dried at 150°C under vacuum for two days.

Ruthenium Insertion into TMP-Zeolite

The preparation procedure was similar to that for inserting metal into the TPP-zeolite, as reported above. To a three-necked round-bottom flask, TMP-zeolite (5 g), $Ru_3(CO)_{12}$ (0.5 g), and dimethyl formamide (DMF; 100 mL dried over a 4-Å molecular sieve) were added. The mixture was heated to reflux for 1 h. The product was washed with water, then methanol, and dried in a vacuum oven at 150°C for two days.

Preparation of Zeolite Encapsulated Cobalt Schiff Base

The zeolite encapsulated [(1,2-diaminopropylene)bis-salicylideniminato]Co(II), CoSalPn/Y, and [N,N'-(1,1,2,2-tetramethylethylene)bis-(4-methoxysalicylidenimi-nato)]- Co(II), CoVan4TMen/Y, were prepared by the same method. A mixture of aldehyde (salicylaldehyde or 4-methoxysalicylaldehyde), amine (1,2 diaminopropane or 1,1,2,2-tetramethylethylene), and cobalt-exchanged zeolite (containing 4.76% cobalt ions) in a 2:1:1 molar ratio was heated in absolute ethanol to reflux for 16 h under inert atmosphere. The product was filtered and washed with dichloromethane until the washing was colorless. The unreacted cobalt ion was exchanged with sodium acetate in ethanol. The resulting zeolite, after filtration, was added to 1-methylimidazole and allowed to stirred overnight. The catalyst was filtered, then dried at 80°C under vacuum. Elemental analysis for cobalt was 0.70% in CoSalPnZL and 1.5% in CoVan4TMenZL.

Preparation of Tetrasulfophthalocyanine (TSPC) Complexes

The procedure was adapted from that reported by Busch and Weber.[35] A mixture of the monosodium salt of 4-sulfophthalic acid (0.2 mol), urea (1.2 mol), ammonium chloride (0.2 mol), ammonium molybdate (0.001 mol), nitrobenzene (100 mL), and the appropriate metal compound (0.06 mol $CoCl_2$, $FeCl_2$, $CuCl_2$, $MnSO_4$, $Ru_3(CO)_{12}$, $Mo(CO)_6$, $PdCl_2$, $PtCl_2$, or $NiCl_2$) was added to a 500-mL, three-necked flask fitted with a reflux condenser and a mechanical stirrer. The mixture was heated slowly to 150°C and maintained there with continuous stirring for 0.5 h until gas evolution ceased. The temperature was then raised to 180°C and maintained at this level for 5 h. After cooling, the solid was filtered, washed with 500 mL of methanol, and added to 1 L of 1 N HCl. The slurry was heated to reflux for 0.5 h. The solid was filtered off, washed with 200 mL water, and dissolved in 1 L of 0.1 N NaOH solution. The solution was then heated at 80°C for 3 h while sodium chloride (300 g) was added slowly. The sodium salt of the TSPC complex precipitated on cooling and after isolation was redissolved in water (1 L). This solution was acidified to pH 2 with 2 N HCl. The resulting precipitate was filtered and dried under vacuum at 80°C overnight to yield the acidic form of the TSPC complex.

Preparation of Magnesium Oxide Supported TSPC Complexes

The metal TSPC complex (0.5 g) was dissolved in DMF (500 mL), then added to MgO powder (10 g) and stirred for 2 h. DMSO was added if the phthalocyanine complex was not

soluble enough in DMF. After washing with DMF until the washings were clear and washing the DMF away with acetone, the catalysts were dried at 60°C under vacuum overnight.

TASK 4: TESTING OF METHANE PARTIAL OXIDATION CATALYSTS

General Procedure for Testing Methane Oxidation Catalysts

We set up a relatively simple isothermal down-flow reactor to test the oxidation catalysts. The catalyst was first heated under argon flow at 200°C to remove vaporizable impurities such as water. The methane used was diluted with 90% helium. The methane and oxygen flow rates were controlled by needle valves, and the exhausted gas was passed through a cold trap (dry ice/ethanol) at -78°C and then through an oil-filled bubbler. A soap-film flowmeter connected to the end of the bubbler checked the flow rate periodically. The liquid collected in the cold trap was allowed to warm to room temperature at the end of the reaction. The methane-to-oxygen ratio was set at 2:1; the total flow rate was 100 mL/min. We used 1 g of catalyst for each run, and each run was monitored for 24 h.

The catalyst (3 g) was loaded into a ss reactor (3/8-in. outer diameter). The reactor was connected to the reactor system and purged with helium for 15 min, then heated to 200°C under a slow flow of hydrogen for 2 h. Methane (10.3% in helium) and oxygen (5.2% in helium) were introduced to the reactor and the temperature was increased to 300°C or higher. Methane and oxygen were individually controlled by mass flow controllers. Reactor pressure was set at 50 psig via a back pressure regulator. A thermocouple was immersed in the catalyst bed and connected to a temperature controller that controlled the furnace. The outlet gases were fed to a GC sampling valve through heated (110°C) ss tubing.

Testing of Methanol Decomposition:

The reactor system used for testing methane oxidation catalysts was modified for the introduction of liquid reagents by adding a length of 1/16-in. ss tubing to the inlet of the reactor. Methanol was fed into the reactor (a 3/8-in. ss tube) via a HPLC pump. Helium gas was added to dilute and carry the methanol through the reactor to the GC. The tubing that connected the reactor outlet and the GC was heated to 110°C to minimize condensation. Methanol decomposition was tested on an empty reactor, MgO (2 g), and Na-Y zeolite (2 g).

RESULTS AND DISCUSSION

This project explored two novel techniques for the conversion of methane to useful products: direct catalytic dehydrocoupling of methane to give hydrocarbons and hydrogen, and oxidation of methane to methanol by using heterogenized versions of catalysts that were first developed as homogeneous models of cytochrome P-450, an enzyme that is active for the hydroxylation of hydrocarbons by using molecular oxygen.

The dehydrocoupling catalysts developed during this project were based on novel surface confined catalysts and were prepared by reacting organometallic complexes of transition metals with inorganic oxide supports to produce surface-confined metal complexes. The increased activity of such highly dispersed catalysts is desirable for activating the relatively inert methane, and highly dispersed catalysts have the additional advantage of resistance to coking. The use of zeolitic supports provides further stabilization of the highly dispersed catalysts, which are confined inside the zeolite pores. The variables we studied include cluster size, support, and reaction conditions.

The oxidation catalysts developed during this project are based on mimics of cytochrome P-450 that have been heterogenized to allow operation in a fixed-bed reactor and to increase stability of the catalyst. Mimics of cytochrome P-450 are macrocylic complexes of transition metals, including porphyrins and phathalocyanines. The variables we studied include the macrocycle, the metal, the support, and the reaction conditions.

TASK 1: SYNTHESIS OF METHANE DEHYDROCOUPLING CATALYSTS

The synthesis of these catalysts involved three steps, as described in detail in the previous section: (1) synthesis of the ruthenium cluster precursors, (2) our novel approach to react the organometallic clusters with alkyl aluminum, and (3) anchoring of these catalysts on supports by a chemical reaction between the hydroxyl groups of the support and the alkyl groups of the organometallic cluster to give a covalent chemical bond.

The organometallic complexes used—a monoruthenium complex, $Ru(allyl)_2(CO)_2$; a tetrameric ruthenium cluster, $H_4Ru_4(CO)_{12}$; a hexameric ruthenium cluster, $H_2Ru_6(CO)_{18}$; a

monomeric ruthenium complex, NaRu (allyl) (CO_3); and a mixed metal cluster, $H_2FeRu_3(CO)_{13}$—were prepared using literature methods.

The tetrahydridoruthenium carbonyl was prepared by a method developed in our laboratories, the direct reaction of triruthenium dodecacarbonyl with hydrogen in hexamethyldisilazane (HMDS) at elevated temperature.

$$4/3\ Ru_3(CO)_{12} + 2H_2 \xrightarrow[135°C]{HMDS} H_4Ru_4(CO)_{12} + 4(CO) \qquad (8)$$

The hydrido complexes reacted readily with triethyl aluminum at room temperature; Equations (9) and (10) are shown as examples:

$$H_4Ru_4(CO)_{12} + Et_3Al \xrightarrow[25°C]{THF} (Et_2Al)Ru_4H_3(CO)_{12} + EtH \qquad (9)$$

$$H_2Ru_6(CO)_{12} + Et_3Al \xrightarrow[25°C]{THF} (Et_2Al)Ru_6H(CO)_{18} + EtH \qquad (10)$$

The reaction stoichiometries were determined by measuring the quantity of ethane produced. These alkyl aluminum carbonyl ruthenium clusters were then used to react with the supports, as shown in Reactions (11) and (12). Three types of supports (β-alumina, 5-Å molecular sieves, and LZ-Y52 zeolite) were used.

$$(Et_2A)Ru_4H_3(CO)_{12} + \text{support-OH} \xrightarrow[25°C]{THF} \text{support-O-Al(Et-}Ru_4H_3(CO)_{12} + EtH \qquad (11)$$

$$(Et_2Al)Ru_6H(CO)_{18} + \text{support-OH} \xrightarrow[25°C]{THF} \text{support-O-Al(Et-}Ru_6H(CO)_{18} + EtH \qquad (12)$$

The reaction stoiciometries for the reaction of the alkylaluminum-cluster complexes with the supports were also determined by measuring the quantity of ethane produced.

The monomeric ruthenium complex reacts directly with the acidic support to release 1 eq. of propylene. The tetraruthenium and mixed iron-ruthenium clusters were also supported on magnesium oxide by the reaction of the acidic hydride and the basic groups on the MgO surface.

TASK 2: TESTING OF METHANE DEHYDROCOUPLING CATALYSTS

The ruthenium catalysts synthesized in Task 1 were tested for activity toward methane dehydrocoupling. Tests were conducted in an isothermal down-flow microreactor. Products of the reaction were determined by GC. The variables studied included temperature, pressure, space velocity, and catalyst.

The results for the ruthenium catalysts are summarized in Table 4. We used a commercial ruthenium catalyst that is supported on alumina (obtained from Engelhard) for comparison. The metal loadings were measured by elemental analysis (Galbraith Laboratory).

Table 4

ACTIVITY OF RUTHENIUM CATALYSTS FOR METHANE DEHYDROGENATION[a]

Catalyst[b]	Ru (wt%)	Flow Rate (mL/min)	Conver. (%)	% Selectivity[c] to H_2	% Selectivity[c] to C_2	% Selectivity[c] to C_6^+
Ru-com	0.50	50	71.2	151.0	--[d]	-
RuAl	0.35	10	3.0	139.9	2.8	-
RuZL	0.31	10	2.3	147.5	1.2	-
RuZL	0.37	10	1.7	177.5	2.6	-
Ru_4Al	0.61	100	10.1	78.6	1.62	-
Ru_4MS	0.49	100	4.9	146.6	3.52	-
Ru_4ZL	0.61	50	1.7	25.3	6.9	28.9
Ru_6Al	1.26	50	6.1	113.4	6.9	41.4
Ru_6MS	0.19	50	5.6	192.8	1.0	14.8
Ru_6ZL	0.20	50	3.6	161.9	3.6	10.0

[a]Reaction conditions: temperature = 750°C, pressure = 150 psig.

[b]Abbreviations: Ru-com = commercial ruthenium catalyst from Engelhard; $Ru_4 = (C_2H_5)_2AlRu_4H_3(CO)_{12}$; $Ru_6 = (C_2H_5)_2AlRu_6H(CO)_{18}$; Ru = Ru(Allyl)$(CO)_2$; Al = b-alumina; MS = 5-Å molecular sieve; ZL = LZ-Y zeolite.

[c]Selectivities were calculated on converted methane. Selectivities to hydrocarbons are based on carbon number.

[d]Not detected.

The effect of reaction temperature was similar for every catalyst. Figure 5 shows the correlation between reaction temperature and methane conversion: higher methane conversion and product yield were obtained at higher temperature. These results were expected, because dehydrocoupling of methane is a thermodynamically unfavored process.[18] Increasing the reaction pressure had a similar effect on the methane conversion, as shown in Figure 6. However, the product selectivities for hydrogen and C_2 hydrocarbons decreased. The selectivities to C_6 or higher hydrocarbons increased with the reaction pressure (Table 5), with the highest selectivity obtained at 150 psig. Because our calculations are based on hydrocarbons containing up to six carbons, significant yields of higher carbon number hydrocarbons will decrease the numeric value. In other words, at higher pressure, the reaction could be producing more high molecular weight hydrocarbon (e.g., C_{10} or higher) than low molecular weight hydrocarbon (e.g., C_6 or C_7). These C_6^+ products need to be separated further to gain a better understanding of the pressure effect. Increasing the space velocity (flow rate) had the opposite effect: the methane conversion significantly decreased but the selectivities to hydrocarbon products increased.

Table 5

EFFECT OF REACTION PRESSURE AND SPACE VELOCITY ON THE ACTIVITY OF Ru_6ZL[a] AT 750°C

Pressure (psig)	Flow Rate (mL/min)	$\%CH_4$ conversion	%Selectivity[b] to		
			H_2	C_2	C_6^+
50	50	3.18	164.16	6.04	6.6
150	50	5.19	91.33	4.48	10.70
250	50	8.64	82.41	2.46	7.38
250	100	2.62	177.10	9.24	20.64

[a] Ru_6ZL = zeolite supported Ru_6 cluster, $C_2H_5AlRu_6H(CO)_{18}$.
[b] Selectivity based on carbon number of hydrocarbon and amount of methane reacted.

Coking is a general problem of heterogeneous catalysts and causes deactivation of the catalyst. The catalytic activities of these ruthenium catalysts as reflected by the methane conversion during a 12-h reaction are shown in Figure 7. The zeolite- and alumina-supported catalysts behaved similarly in that the methane conversion decreased during the first 2 h of reaction and then reached a steady state. The 5-Å molecular-sieve-supported Ru_6 catalyst had a very high methane conversion

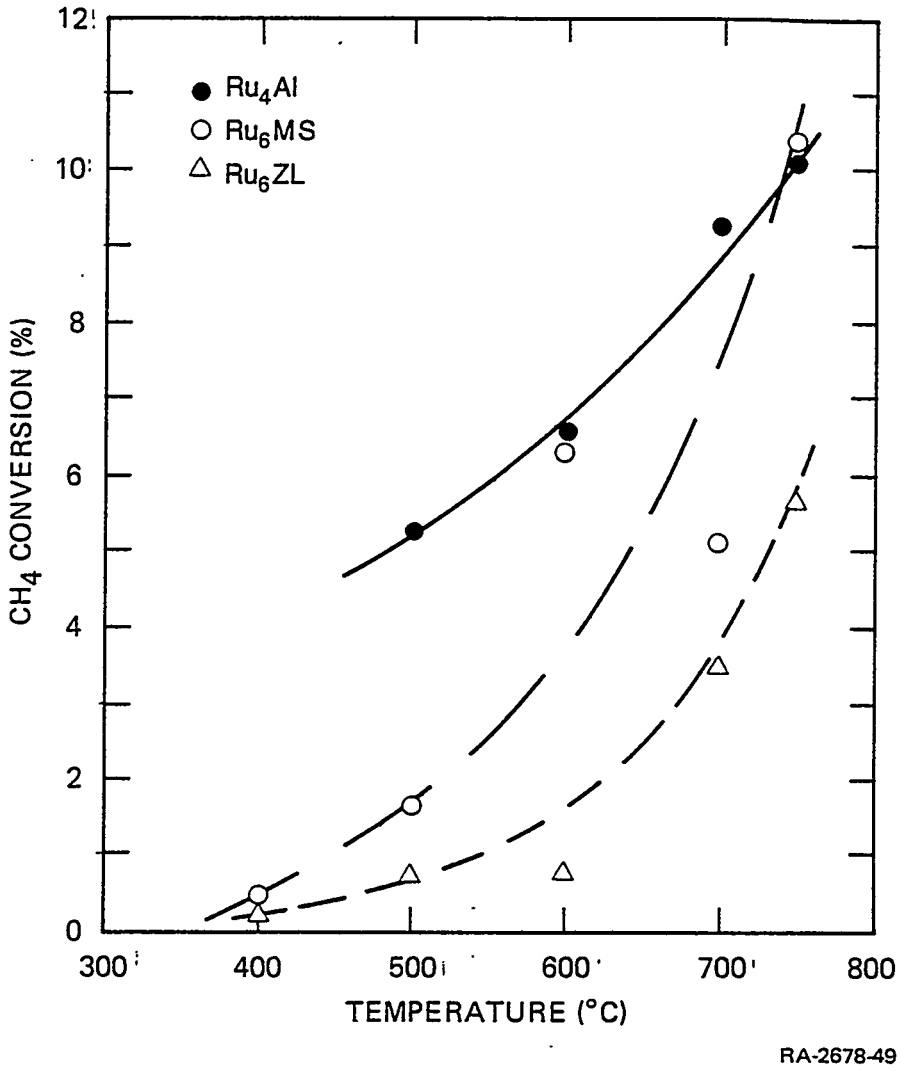

Figure 5. Correlation of reaction temperature and percent methane conversion.

Reaction conditions: pressure = 50 psig, flow rate = 50 mL/min.

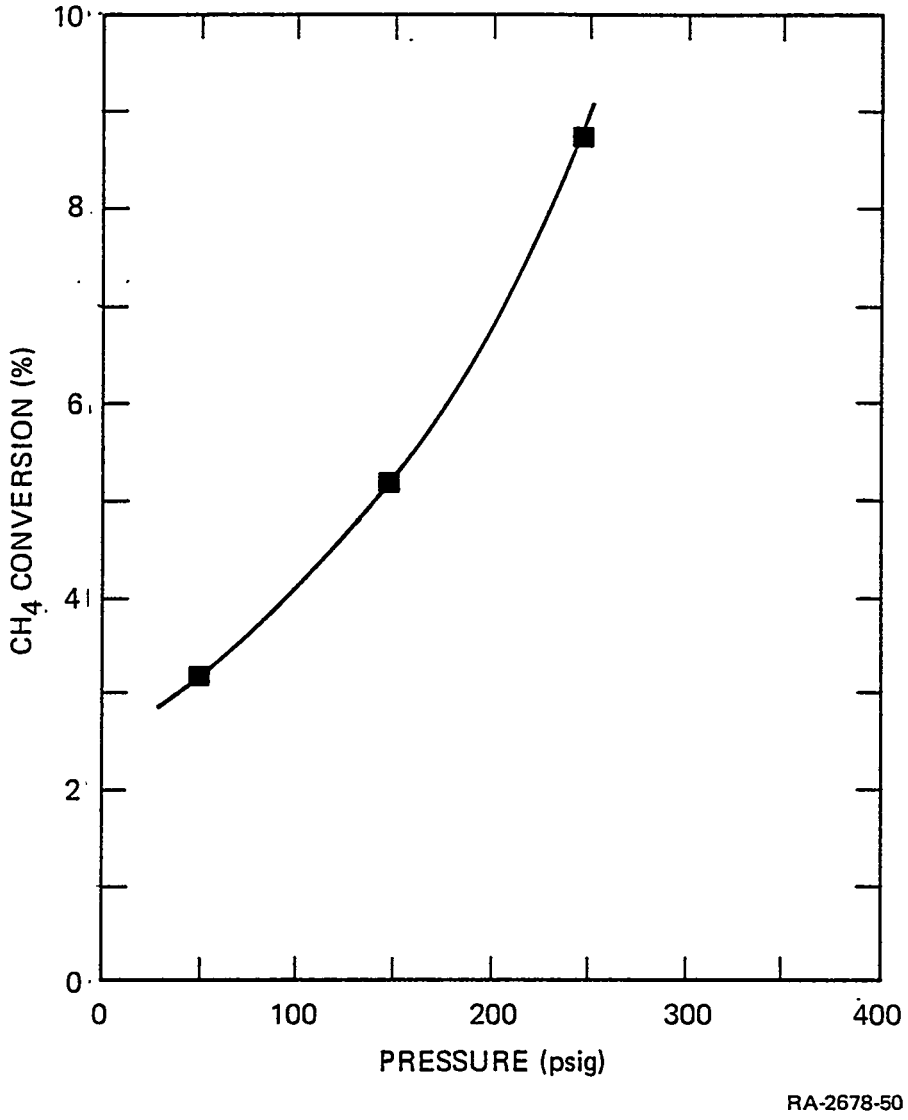

Figure 6. Correlation of reaction pressure and percent methane conversion on Ru_6ZL catalyzed methane reforming.

Reaction conditions: temperature = 750°C, flow rate = 50 mL/min.

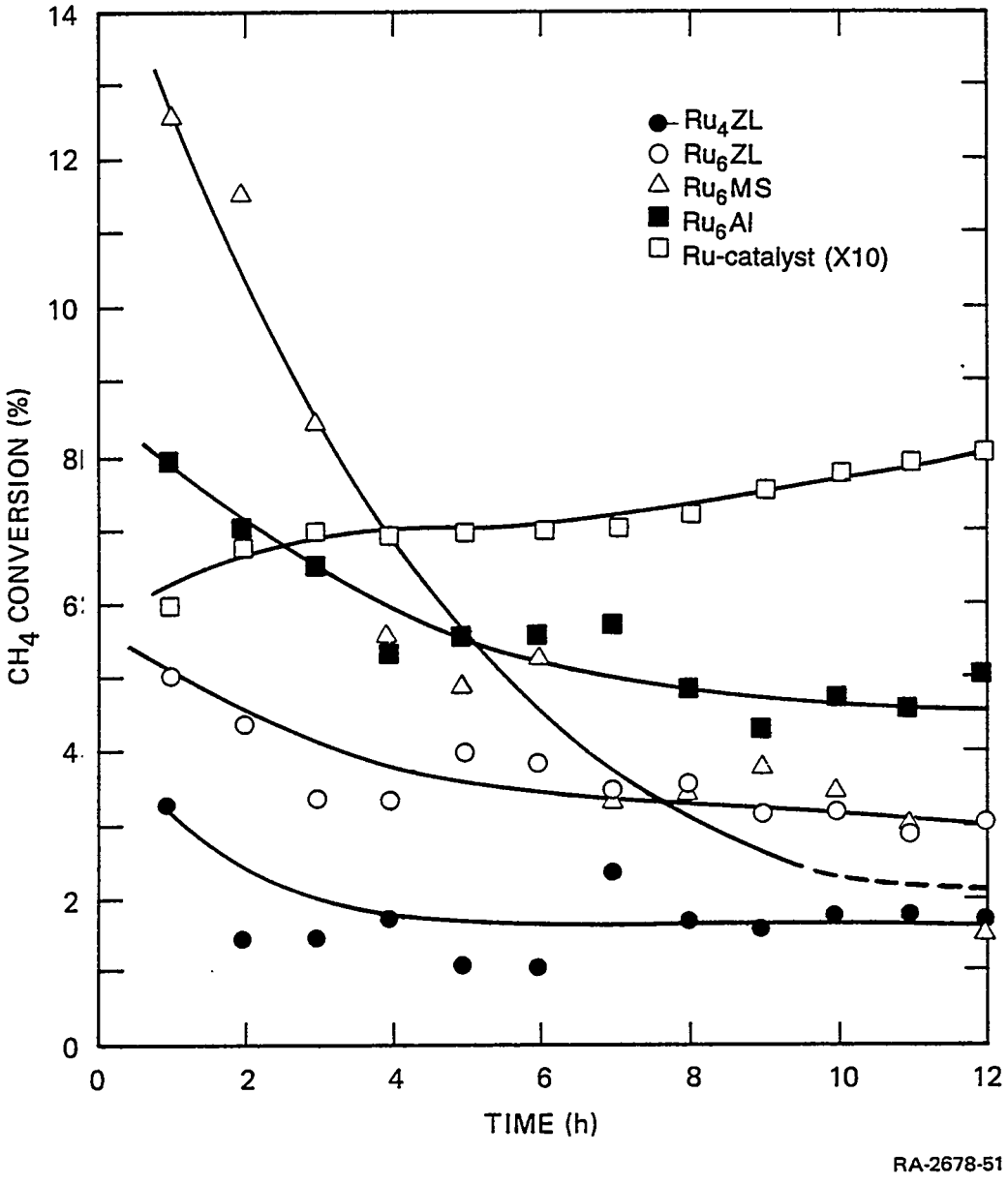

Figure 7. Percent methane conversion as a function of time during a 12-h reaction.

Reaction conditions: temperature = 750°C, flow rate = 50 mL/min.

at the beginning of the reaction, but its activity decreased gradually. The commercial ruthenium had a totally different activity: its methane conversion was about ten times higher than that of our Ru clusters, and its activity slowly increased during the reaction. These results were confirmed by the elemental analysis which shows carbon accumulation during the reaction (Table 6).

Table 6

ELEMENTAL ANALYSES OF RUTHENIUM CATALYSTS FOR METHANE REFORMING[a]

	Before Reaction			After Reaction		
Catalysts	**%C**	**%H**	**%Ru**	**%C**	**%H**	**%Ru**
Ru_4Al	5.09	1.04	0.61	26.50	0.40	0.57
Ru_4MS	1.46	1.13	0.49	4.38	0.46	0.64
Ru_4ZL	5.25	1.53	0.61	0.58	0.22	1.26
Ru_6Al	9.77	1.84	1.26	23.24	0.67	0.55
Ru_6MS	0.95	1.68	0.19	22.29	0.19	0.32

[a]Reaction with methane at 750°C for 15 h.

Our intention in using different supports was to confine the ruthenium cluster at different locations on or within the support. Hence, the Ru_4 and Ru_6 clusters were dispersed on the alumina surface but confined inside the pores of zeolitic supports. The pore size of 5-Å molecular sieves is too small for the Ru_6 cluster but was expected to be large enough for the Ru_4 cluster after decomposition. We expected different reactivity for the clusters on different supports. Our results (summarized in Table 4) show that the alumina-supported Ru_4 and Ru_6 clusters gave a higher methane conversion than the same cluster on the other two supports. The commercial ruthenium catalyst was a monoruthenium unit, which should have a higher dispersion. Indeed, it had a much higher methane conversion rate than the Ru clusters. The methane conversions of the zeolite-supported catalysts were lower than those of the other catalysts, a finding suggesting that the Ru clusters were located inside the zeolite cage. The rate of the reaction was determined by the rate of methane entering the zeolite cage and/or the rate of product escaping from the zeolite cage.

The size of the cluster (e.g., Ru_4 vs Ru_6) also affected the methane conversion and the product yield. In the cases of molecular sieves and zeolite supports, the Ru_6 cluster had higher

activity than the Ru_4 cluster. The results on alumina supports were different, probably because of the higher dispersion of the smaller cluster. Since our results on the Ru_4Al and Ru_4MS were averaged from 2-h reactions and the others were averaged from 12-h reactions, these data may not be reliably compared. Further studies on the cluster size effect are planned.

In summary, our results show that these organometallic-drived ruthenium clusters are effective in dehydrocoupling methane. Although the methane conversion ranges from 1.74 to 10.11%, much lower than with the commercial ruthenium catalyst, the commercial ruthenium catalyst produces only trace amounts of C_2 hydrocarbon and no higher hydro-carbons, apparently forming coke. Therefore, the commercial catalyst is not useful for our purpose. Our ruthenium catalysts produce considerably more of the higher hydrocarbons (C_2 and C_6 or higher). A very small amount of CO_2 is also produced in these reactions and is probably due to impurities (e.g., oxygen) in the gas cylinder.

Most of the reports on catalytic conversion of methane to higher hydrocarbons are based on metal oxides using the oxidative coupling pathway. Few examples have been reported on direct methane reforming. Table 2 lists some of the literature results on both oxidative coupling and reforming, including our results.[24] It is difficult to truly compare the catalytic activities of the catalysts because the experimental conditions are so different. However, on the basis of methane conversion and the selectivities for higher hydro-carbons, our catalysts are comparable. We believe the catalytic activities of our ruthenium catalysts can be improved by proper modification of the reaction conditions. Generally speaking, oxidative coupling of methane gives only C_2 hydrocarbons, but methane reforming gives higher molecular weight hydrocarbons (C_6^+) in addition to the C_2 hydrocarbons. None or very small amounts of C_3-C_5 hydrocarbons have been detected. Mitchell and Waghorne[19] reported that the major product of alumina-supported CaCrPt catalyst under anaerobic condition is benzene. Jones and Sofranko[20] also observed small amounts of benzene produced from methane reforming over silicon-supported GeO_2. We have not yet identified our C_6^+ product, but it is possible that it contains benzene.

We also tested three of the catalysts supported on a basic support (MgO). The results are presented in Table 7. At the same reaction temperature, the magnesia supported tetraruthenium cluster gave a higher hydrocarbon yield (but a lower methane conversion) than the zeolite supported tetraruthenium cluster. The catalysts contained 0.25% ruthenium for Ru_4MgO and 0.14% for Ru_4ZL. The difference in reactivity may result from the difference in metal loading as well as in the type of support. Methane conversion is much higher with the magnesia supported ruthenium monomer. However, the product selectivity is lower.

Table 7

CATALYTIC REACTIVITY OF ZEOLITE AND MAGNESIA SUPPORTED CATALYSTS FOR METHANE REFORMING[a]

Catalyst	Temp (°C)	Methane Conversion (%)	Selectivity (%)[b]	
			C_2	C_{6+}
Ru_4ZL	750	6.07	0.9	2.5
Ru_4MgO	750	4.04	6.9	49.2
RuZL	750	1.7	2.6	--[c]
RuMgO	600	21.044	0.1	0.5
$FeRu_3ZL$	600	3.07	1.9	18.5
$FeRu_3MgO$	600	8.87	0.1	--

[a]Reaction conditions: pressure = 150 psig, flow rate = 20 mL/min, weight of catalyst = 2 g, ss reactor O.D. = 3/8 in.
[b]Selectivity to hydrocarbon is based on carbon number.
[c]Not detected.

A mixed metal cluster of iron and ruthenium ($FeRu_3$) was also studied, and the results are presented in Table 7. Introduction of the iron to the metal cluster is advantageous to methane dehydrogenation activity. At 750°C, 23.5% of the methane was converted over $FeRu_3ZL$ while only 6% was converted with Ru_4ZL (see Figure 8). However, the hydrocarbon yield was reduced under those conditions. At lower temperature (600°C, where Ru_4ZL was inactive), the mixed metal cluster on zeolite gave 3% conversion and reasonable hydrocarbon yields. Supporting the mixed metal cluster on magnesia resulted in higher activities and lower hydrocarbon yields.

At 750°C, the mixed metal cluster was ten times more active than the Ru_4 cluster (41.5% methane conversion by the $FeRu_3$ cluster compared with 4.0% methane conversion by the Ru_4 cluster). We therefore investigated the behavior of these two systems under flow-through conditions by infrared spectroscopy using diffuse reflectance (DRIFT). The DRIFT cell can be heated to operating temperatures as a means of determining the source of the differences in activity between the catalysts.

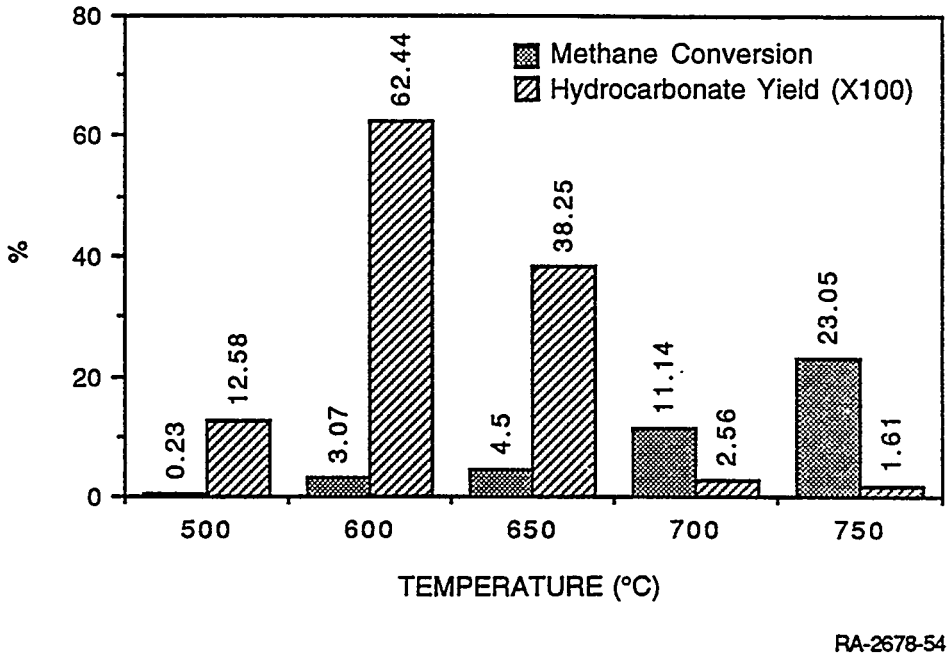

Figure 8. Effects of temperature on methane conversion and hydrocarbon yield of $FeRu_3ZL$.

Under nitrogen, we observed large differences in the spectra of these two supported clusters on magnesia at room temperature (Figure 9). The spectrum we obtained for the Ru_4 cluster on magnesia is very similar to that obtained by Vichiyama and Gates for $H_4Ru_4(CO)_{12}$ adsorbed onto magnesia and treated with helium at 100°C[110]: two broad peaks of equal intensity at about 2038 and 1965 cm^{-1}. Starting with $Ru_3(CO)_{12}$ and MgO, Guglielminotti obtained the same spectrum.[111] On alumina,[112] an additional small peak was observed at about 2000 cm^{-1}. The close resemblance of these four spectra is somewhat surprising. Vichiyama and Gates proposed that $H_4Ru_4(CO)_{12}$ reacts with the basic magnesia surface by deprotonation to give the anion $[H_3Ru_4(CO)_{12}]^-$ and hydrogen.[110] The similarity of the spectrum suggests that rearrangement of the various starting clusters has occurred to give similar surface species. As an example, such rearrangement under mild conditions has been observed for $Ru_3(CO)_{12}$ on magnesia surfaces: a molecule of carbon dioxide is released, and the cluster $[HRu_3(CO)_{11}]^-$ is formed on the surface.[113]

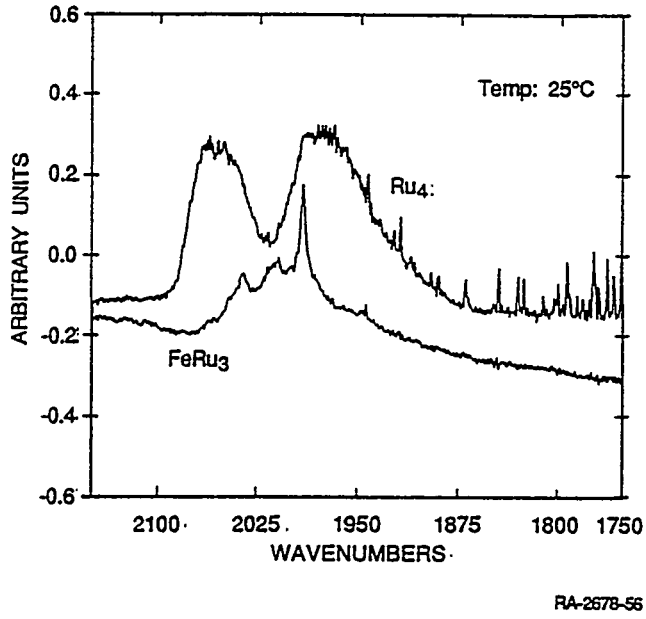

Figure 9. Comparison of Ru_4 and $FeRu_3$ clusters on MgO under N_2.

The spectrum of the mixed metal cluster in Figure 9 is more complex. At least three peaks are observed, at 2035, 2005, and 1975 cm^{-1}. This spectrum is similar to that obtained by Basset's group on reacting $H_2FeRu_3(CO)_{13}$ with hydrated magnesia,[114] although our spectrum has a more intense peak at 1975 cm^{-1}. In both cases the peak due to a bridging carbonyl at about 1820 cm^{-1} is not observed. $Fe_2Ru(CO)_{12}$ and $H_2FeRu_3(CO)_{13}$ on alumina also give spectra identical to each other.[115] Basset's group has shown that the major species on the magnesia surface is the anion $[HFeRu_3(CO)_{13}]^-$, obtained by extraction with PPNCl in dichloromethane.[114]

The spectrum of $FeRu_3$/MgO changes as the sample is heated above 100°C. At 200°C, a broad featureless peak is observed centered at about 1980 cm^{-1} (Figure 10). By 300°C, this feature is barely observable (Figure 11). Basset and coworkers found that the $[HFeRu_3(CO)_{13}]^-$ cluster on magnesia produced several moles of hydrogen per cluster when heated over 100°C.[114] The origin of this hydrogen was proposed to be the water-gas shift reaction between carbon monoxide and surface water. The final product was small metal particles. On alumina, decomposition of samples prepared with $Fe_2Ru(CO)_{12}$ first produced $Fe(CO)_5$ and then $Ru_3(CO)_{12}$.[116] The presence of iron accelerates the decomposition of the ruthenium cluster when the iron and ruthenium are absorbed together.[117] In our case, the source of water for the water-gas shift reaction is more problematical. The magnesia was heated to 450-500°C under flowing nitrogen, then placed in the dry-box. The solvents used in the deposition reactions were all dried before use. For the IR studies, the samples were loaded into the IR cell in the dry-box and the cell was then sealed.

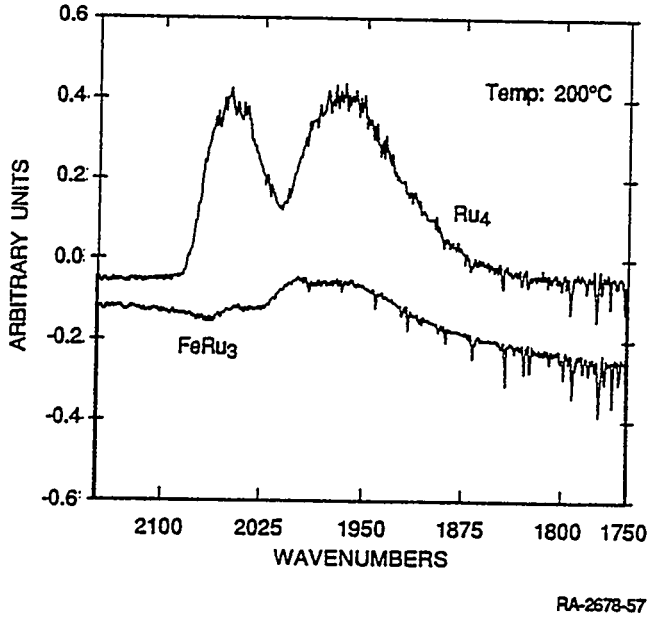

Figure 10. Comparison of Ru_4 and $FeRu_3$ clusters on MgO under N_2.

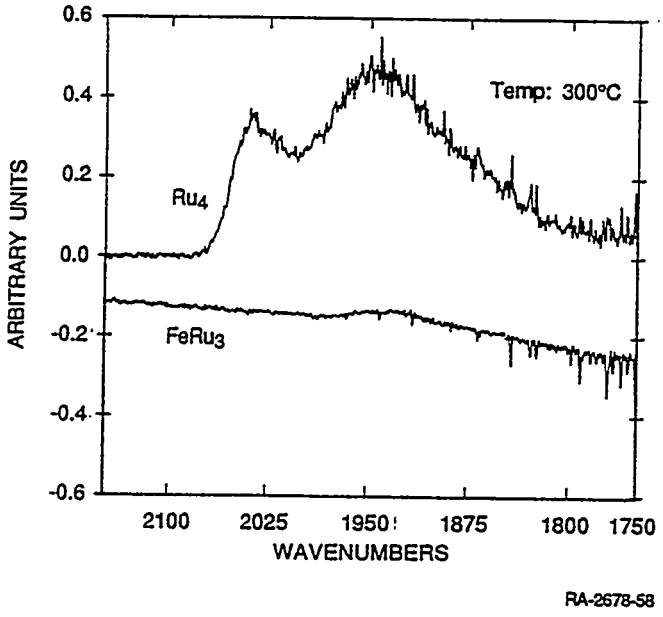

Figure 11. Comparison of Ru_4 and $FeRu_3$ clusters on MgO under N_2.

The Ru_4/MgO catalyst, in contrast, is unchanged at 200°C. At 300°C (Figure 11) the intensity of the upfield peak has begun to decline. Both peaks have also shifted by about 10 wavenumbers to a longer wavelength. At 400°C, the higher wavenumber band has disappeared (Figure 12) and the other peak has declined in intensity and shifted to about 1905 cm^{-1}. Further heating of the sample caused this peak to continue to decline in intensity and shift to lower wavenumbers. By 600°C, only a very broad peak is observed at about 1880 cm^{-1}. This behavior is similar to that observed by Guglielminotti with a sample of ruthenium metal prepared from $Ru_3(CO)_{12}$ and magnesium hydroxide.[111] In this case, the shift in the peak arises from an annealing process. The results from these studies under nitrogen show that the mixed metal cluster decomposes at lower temperature; this parallels the greater activity of this catalyst system in the methane dehydrocoupling reaction. The greater activity of the mixed metal system may also be due to the presence ofiron influencing the morphology of the ruthenium metal particles formed.

We next examined the behavior of the Ru_4MgO catalyst under methane. We used 5% methane in argon for these experiments. A comparison of the two spectra in the carbonyl region (under nitrogen and methane) is shown in Figure 13. Both the relative peak positions and intensities are identical. Heating the Ru_4MgO catalyst under methane produced the same behavior in this region as was seen under nitrogen (described above); this can be seen in Figure 12, which compares the spectra obtained at 400°C. In both cases, a slight shoulder is observed at about 2000 cm^{-1}, while the major peak is very broadly centered at 1935 cm^{-1}. Examination of the spectra in the C-H region shows that under methane the absorbency of methane was greater for the MgO blank at room temperature. Two bands are observed at 2920 and 2850 cm^{-1}. These peaks did not change in relative position or intensity until over 600°C, when they were no longer observed.

We also studied the behavior of the mixed metal cluster when heated under methane. A comparison of the $FeRu_3/MgO$ catalyst under nitrogen and under methane at 25°C is shown in Figure 14. The spectrum under nitrogen was described above. Under methane, a very large absorption is observed between 2050 and 1940 cm^{-1}; there is a great deal of fine structure on this peak, which suggests that a large number of species have been formed. This absorption is attributed to mobile subcarbonyls that arise from decomposition of the cluster.[114,118] When $FeRu_3/MgO$ is heated under nitrogen, the absorption due to carbonyl bands practically disappears between 100° and 200°C. By 300°C, no absorption bands are observed (Figure 15). Under methane, peaks are observed in the carbonyl region for this system. At 300°C, a peak is observed at 2030 cm^{-1}, along with a broader peak at about 1950 cm^{-1}. Both the peak positions and relative intensities match the spectrum observed for Ru_4/MgO (Figure 11) under nitrogen or methane.

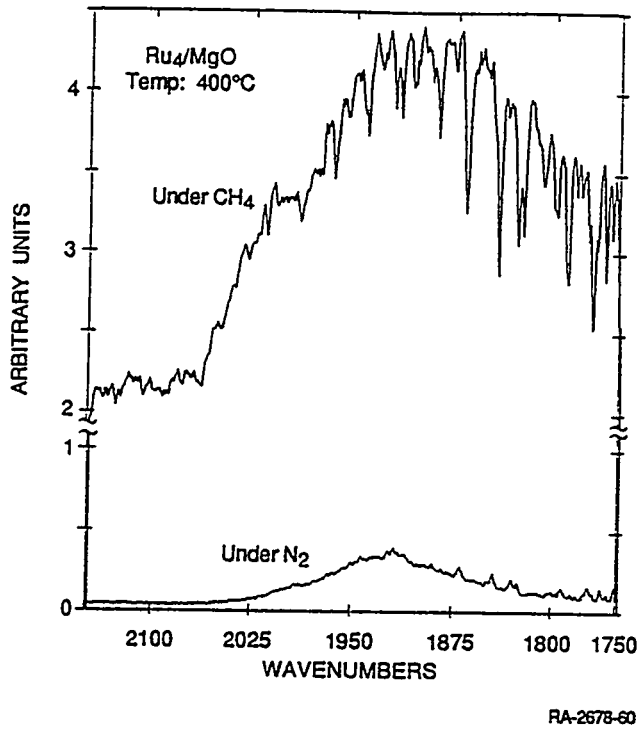

Figure 12. Comparison of Ru_4 clusters on MgO under CH_4 and N_2.

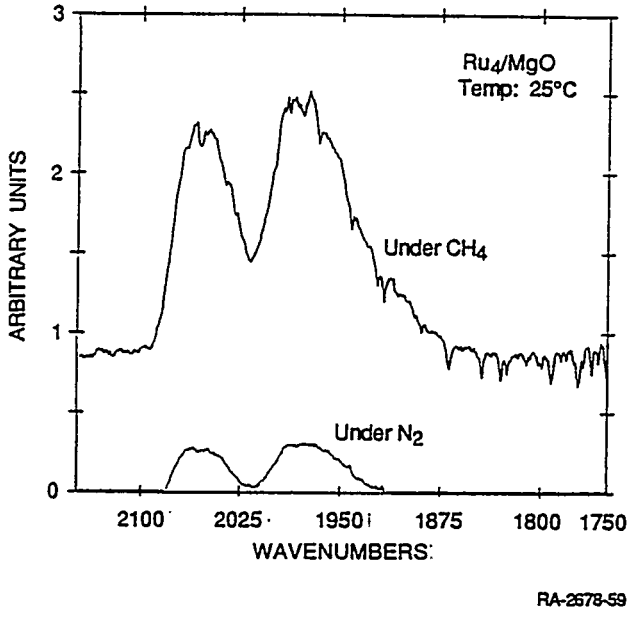

Figure 13. Comparison of Ru_4 clusters on MgO under CH_4 and N_2.

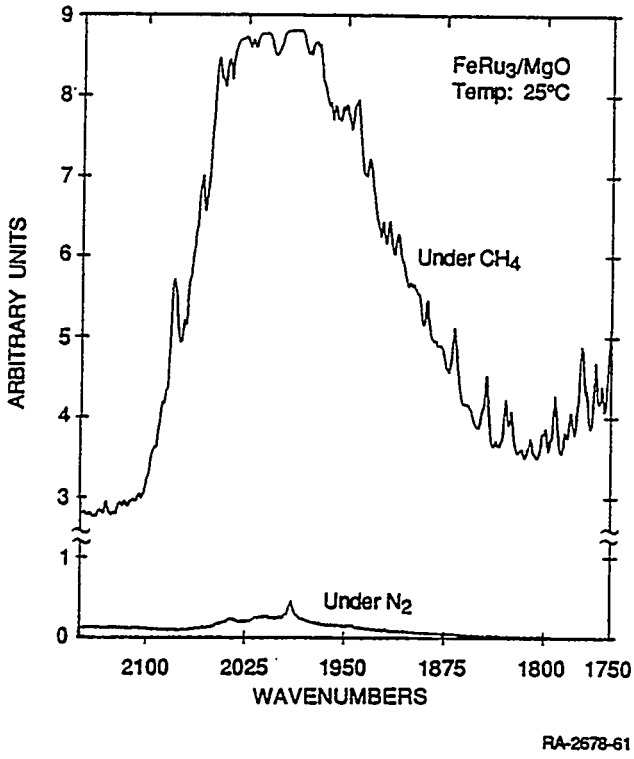

Figure 14. Comparison of Ru_4 clusters on MgO under CH_4 and N_2 at 25°C.

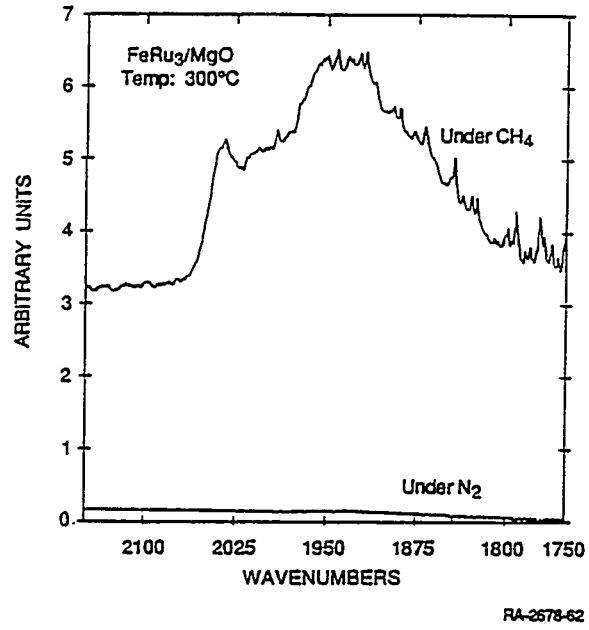

Figure 15. Comparison of Ru_4 clusters on MgO under CH_4 and N_2 at 300 °C.

These similarities indicated that the mixed metal cluster has decomposed under methane and segregated into separate iron and ruthenium species. Guczi and coworkers observed a similar segregation on alumina.[118] Upon further heating, the species derived from $FeRu_3/MgO$ behaves exactly like Ru_4/MgO. By 400°C, the higher wavenumber band has disappeared, and the lower wavenumber band has shifted slightly lower (Figure 16). By 600°C, no bands are observed in the carbonyl region. The difference in the behavior of the $FeRu_3/MgO$ system under nitrogen and methane is very surprising, especially since we have not observed such differences with the Ru_4/MgO system. Apparently the decomposition of the $FeRu_3/MgO$ system gives some very active ruthenium species that can interact with methane and promote further segregation of the two metals. The iron present in this system may undergo a disproportionation reaction to give some volatile iron carbonyls and some iron ions that can act as nucleation centers for ruthenium clusters. These species may have different morphologies and thus different catalytic properties.

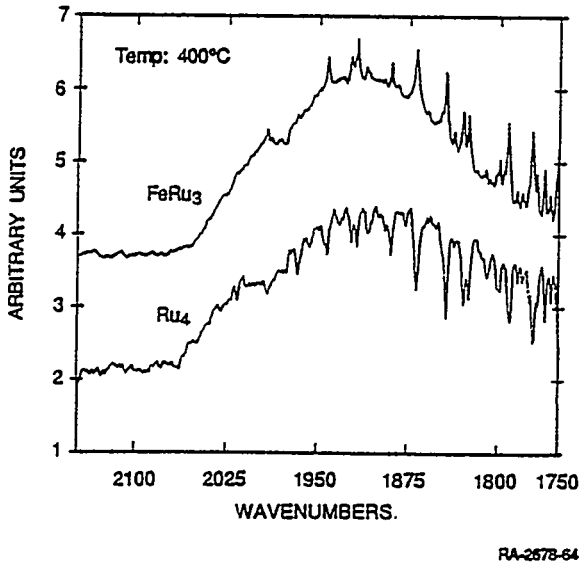

Figure 16. Comparison of Ru_4 and $FeRu_3$ clusters on MgO under CH_4.

We also investigated the use of a membrane reactor to drive the reaction by removing hydrogen. We designed a reactor, as shown in Figure 1, that has the catalyst packed around a Pd/Ag membrane tube. Hydrogen formed from the methane dehydrocoupling diffuses into the Pd/Ag tube because of the partial pressure differential. Hydrogen was successfully removed in a test experiment with the ruthenium catalyst, as evidenced by GC analyses. However, a leak quickly developed. We then redesigned the reactor as shown in Figure 2. This reactor was successfully used in a 72-h run (results shown in Table 8). Unfortunately no evidence of enhanced methane conversion or

hydrocarbon selectivity was observed. This result implies that the reaction is not equilibrium limited under these conditions.

Table 8

EFFECTS OF HYDROGEN PARTIAL PRESSURE AND SUPPORTS ON THE CATALYTIC REACTIVITY OF REFORMING CATALYSTS AT 750°C

Catalyst[a]	Methane Conversion (%)	Selectivity[b]		
		H_2(%)	C_2(%)	C_6^+
Ru_4ZL	6.07	99.0	0.89	2.5
Ru_4ZL/Pd-Vacuum	5.27	8.5	0.76	4.3
Ru_4ZL/Pd-He flow	5.34	77.9	0.79	2.9
Ru_4ZL-5 g	43.11	98.7	0.28	0.7
Ru_4MgO	4.04	42.82	6.88	49.2

[a]Ru_4Al/Pd is the reaction using the Pd/Ag membrane.
[b]Selectivity for hydrocarbons is based on carbon number.

TASK 3: SYNTHESIS OF METHANE PARTIAL OXIDATION CATALYSTS

The systems we synthesized and examined for activity in the partial oxidation of methane consist of metalloporphyrins and metallophthalocyanines, either encapsulated in the pore structure of a zeolite or attached to an inorganic oxide support. Metalloporphyrins especially have been widely examined as alkane oxidation catalysts in homogeneous or two-phase liquid systems.[44] The lifetime of these systems is usually short, since the catalyst degrades readily under the oxidizing conditions. One of the most common degradation pathways is the formation of oxygen bridged dimers such as the μ–oxo species [M]–O–[M] (where [M] represents the metalloporphyrin), which is inactive for further reactions with oxygen and/or the hydrocarbon.

One of the best ways to prevent formation of this degradation product is to immobilize the oxidation catalyst on a surface. The reduced mobility of the catalyst makes it less likely that two of the catalyst monomers will react to form the inactive dimer. This immobilization can be accomplished in several ways. One way is to take advantage of the metal's ability to form coordinate covalent bonds with electron pair donors (such as amines or phosphines). Compounds containing these ligands are first bound to the surface by a hydrolysis reaction, and then the metal

complex is absorbed from solution by formation of the ligand-metal bond. This approach has been used to form more stable oxygen-carrier systems.[3b] However their use in methane oxidation systems is limited because such a reaction demands a higher temperature at which the complex can dissociate and decompose.

A more effective way to immobilize the metallophthalocyanine species is to encapsulate it in a large pore, such as in a large pore zeolite.[120] This strategy provides two ways to prevent the dimerization leading to degradation: only one complex can fit into the pores of the zeolite at a time, and the openings to these pores are too small for the complex to diffuse out. Another advantage of encapsulating the metallophthalocyanine is the possibility of the zeolite framework imposing selectivity on the oxidation reaction in much the same way as the protein structure does in the reactions of cytochrome P-450. Workers at DuPont have synthesized iron(II) phthalocyanine (FePC) in the large pore Zeolites X and Y and studied its performance in the oxidation of alkanes at room temperature with iodosobenzene as oxygen source.[121] They found that systems with higher loadings of FePC had lower turnover numbers, which they attributed to the blocking of interior sites by FePC complexes situated in pores closer to the exterior of the zeolite.

Encapsulated phthalocyanine complexes are synthesized by direct condensation of four molecules of phthalonitrile around the metal in much the same way the metallophthalocyanine itself is synthesized (Reaction 13).

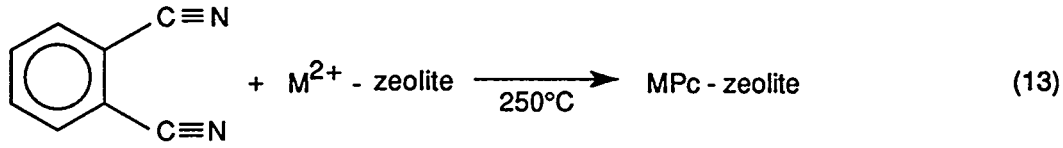

(13)

The only difference is that the source of the metal is an ion-exchanged zeolite rather than a simple metal salt. We used zeolite Y because of its greater ratio of silica:alumina. This ratio is important for two reasons. Lower ratios mean that there is less ion-exchange capacity and that the zeolite is less hydrophilic. This latter quality may be important in trying to observe alcohols directly in the oxidation reactions. Both Wohrle and coworkers[120] and Herron[121] have noticed that the water content of the zeolite is important for this synthesis to succeed. They postulated that protons arising from this water are necessary to replace the metal ion as the charge compensator for the zeolite framework. Successful formation of the encapsulated metallophthalocyanine (MPC/Y) is indicated by the blue-green coloration typical of the phthalocyanine species. In our investigation of zeolite-

encapsulated porphyrin and phthalocyanine complexes for the oxidation of methane to methanol, [33] we observed methanol formation with ruthenium phthalocyanine, cobalt tetraphenylporphyrin, and manganese tetraphenylporphyrin at 375°C (Table 1). The iron and cobalt analogs did not produce methanol under the same conditions. However, it was recently reported that a nitro-substituted iron porphyrin catalyzes conversion of methane to methanol.[34] Thus, the catalytic reactivity of the metal complexes could be enhanced by addition of electron-withdrawing groups to the macrocyclic ligand. Phthalocyanine on the exterior surface of the zeolite was removed by Soxhlet extraction so that the oxidative reactivity would not be dominated by this more accessible material. As shown in Table 9, this washing removed a great deal of material.

Table 9

ELEMENTAL ANALYSES OF OXIDATION CATALYSTS ENCAPSULATED IN ZEOLITE Y

	Before Washing			After Washing with Pyridine		
	%C	%H	%Metal	%C	%H	%Metal
CoPC	14.53	1.59	1.96	2.45	1.66	1.81
FePC	15.61	1.80	1.19	5.95	2.45	0.85
RuPC	17.35	1.87	1.58	7.16	2.06	0.40

After the Soxhlet extraction, we treated the MPC/Y with a solution of sodium acetate or sodium chloride (sodium being the original counter-ion for the zeolite framework). This back-ion-exchange removes any of the metal that is not complexed by the phthalocyanine. The decrease in metal ion content is shown in Table 10. The lack of decrease of iron in the FePC/Y system may be due to formation of an insoluble iron oxide from uncomplexed iron(II) before it can be exchanged with the sodium ion solution.

At this point, the only metal containing species should be MPCs encapsulated in the large pores of the zeolite, so the oxidation activity can be attributed to this species alone. In some cases, these MPC/Y systems were then treated with an excess of pyridine or imidazole, to form adducts with the MPC.

Table 10

ELEMENTAL ANALYSIS OF METHANE OXIDATION CATALYSTS

Catalyst[a]	%Carbon	%Hydrogen	%Nitrogen	%Metal
CoPC/Y-b	14.49	2.56	4.49	2.56
-c	12.14	1.43	3.43	1.53
FePC/Y-b	11.46	1.79	3.04	4.08
-c	8.06	1.51	1.98	4.15
RuPC/Y-b	4.64	2.51	0.64	0.82
-c	2.30	1.68	0.42	0.97
MnPC/Y-b	10.50	2.06	2.75	2.74
-c	9.31	1.42	2.39	1.62

[a]PC = Phthalocyanine, Y = zeolite Y.

[b]Before sodium ion exchange.

[c]After sodium ion exchange.

We used these same methods to synthesize derivatized phthalocyanines encapsulated by zeolite Y. We worked with two such derivatives. In one, the four hydrogens on the phthalonitrile were replaced by four fluorine atoms. In the other derivative, one of the two hydrogens non-adjacent to the nitrile groups was replaced by a sulfonic acid group. We successfully synthesized the CoTSPC/Y species by substituting cobalt-exchanged zeolite as the source of the metal ion in the procedure given by Busch and Weber.[122] A similar reaction to form the corresponding iron species was unsuccessful, most likely because of prior oxidation of the iron(II) to unreactive iron(III) oxide.

We made several attempts to synthesize encapsulated perfluorophthalocyanines (MPFPC/Y). These systems were of interest to us because work with homogeneous porphyrin systems showed that substituting an electron-withdrawing group such as fluorine for hydrogen on the porphyrin led to more active oxidation catalysts which resisted degradation better.[123] Reports on perfluorinated phthalocyanines also suggested that these derivatives had greater stability under oxidizing conditions than the simple underivatized phthalocyanine.[124] We made several attempts (varying temperature, water content, time of reaction) to synthesize the encapsulated versions of both Ru- and CuPFPC. In all cases we obtained a green zeolite, but UV-VIS spectra of extracts

from this substance, when compared to spectra from authentic samples, showed that this substance did not contain any of the perfluorinated phthalocyanine.

The lack of success in forming encapsulated MPFPC/Y is especially frustrating in view of the ease with which the perfluorinated phthalocyanines can be synthesized without the zeolites. A likely explanation for this lack of success is that the PFPC is too big to fit into the large pore of zeolite Y. Herron[121] has shown (by X-ray crystallography) that the encapsulated FePC in a Y zeolite has about a 20° bend instead of being strictly planar. The hydrogens on the perimeter of the phthalocyanine also protrude out of the pore into the channels. Substituting the hydrogens with fluorines adds approximately 1 Å to the diameter of the phthalocyanine molecule, and this extra length can only be accommodated by more severe bending of the complex or by the fluorines protruding a larger distance into the pore. Apparently these distortions are too great to permit formation of the encapsulated PFPC. The larger size of the fluorine also affects the accessibility of the tetrafluorophthalonitrile to the pore itself. The kinetic diameter of the channel leading to the pore is 7.4 Å in unexchanged zeolite X or Y; after exchange with ruthenium or another transition metal, this diameter may be reduced. We calculated the dimensions of the tetrafluorophthalonitrile as being 7.5 by 7.0 Å (phthalonitrile itself having dimensions of 7.1 by 6.2 Å). Thus, it is much more difficult for the tetrafluorophthalonitrile to enter the large pore, especially after the phthalocyanine ring is partly formed in the pore by preceding molecules.

Porphyrins encapsulated in the large pore of a zeolite have not, to the best of our knowledge, previously been reported in the literature. As with the metallophthalocyanines, metalloporphyrins are too large and inflexible to synthesize first and then exchange into the pore. We therefore first tried the synthesis of the metalloporphyrin—in this case, the tetraphenylporphyrin (TPP)—by the template method. The metal of interest is first ion-exchanged into the zeolite, and then this zeolite is heated with pyrrole and benzaldehyde in refluxing DMSO. Encapsulated MTPPs were not obtained by this method.

We then tried another synthetic route. We first synthesized the metal free ligand inside the zeolite cage by refluxing benzaldehyde, pyrrole, and the sodium zeolite (without metal exchange) in acetic acid. This is the method most commonly used to synthesize the porphyrin ligand itself. The resultant zeolite powder, after washing with methanol, appeared purple, an indication of the successful formation of TPP. The washing also contained TPP, as indicated by its UV-VIS spectrum. The desired metal ion was then inserted into the porphyrin by boiling the metal salt and the zeolite containing TPP in DMSO. The product was washed with water and then Soxhlet extracted with methanol to remove surface-bound TPP complex. Uncomplexed metal ions were

removed by reverse ion-exchange as described above. If an axial base is desired, then the MTPP/Y is stirred with a solution of N-methyl-imidazole for 2 h, washed with acetone to remove excess, and dried in vacuum overnight. Four different metal TPP complexes were prepared: Co, Fe, Ru, Mn. The percent complex loadings of these porphyrin catalysts were much lower than those of the phthalocyanine catalysts (Table 11). The main reason was the low yield of ligand synthesis, which was generally around 20%. Iron does not back-exchange well, most likely because of the formation of insoluble iron oxide. The drastic decrease in metal content (compared to carbon, hydrogen, or nitrogen content) for the Co- and MnTPP systems after washing suggests that the insertion reaction with these metals was not very successful, since a porphyrin should not lose its metal under such mild conditions of exchange.

Table 11

ELEMENTAL ANALYSIS OF TETRAPHENYLPORPHYRIN CATALYSTS

Catalyst[a]	%Carbon	%Hydrogen	%Nitrogen	%Metal
CoTPPZL-b	3.93	2.24	1.29	3.83
-c	2.36	1.01	0.41	0.15
FeTPPZL-b	3.66	2.43	1.29	3.83
-c	2.36	1.04	0.48	4.04
RuTPPZL-b	3.44	2.09	0.69	0.27
-c	2.46	1.13	0.52	0.13
MnTPPZL-b	8.33	2.24	1.03	1.42
-c	4.96	1.22	0.58	0.12

[a]Pc = phthalocyanine, TPP = tetraphenylporphyrin, ZL = zeolite.
[b]Before sodium ion exchange.
[c]After sodium ion exchange.

We also synthesized zeolite encapsulated tetramesitylporphyrin (TMP). Since mesitylaldehyde is larger than the benzaldehyde used in the TPP synthesis, more forcing conditions were used. Zeolite powder, zinc acetate, mesitylaldehyde, pyrrole, and pyridine were sealed in a glass reactor under oxygen atmosphere and heated at 180°C for 48 h. Zinc was added to serve as the template and was easily exchanged after the synthesis. After washing with a large amount of acetone, the zeolite was still coated with ZnTMP which could be washed off by chloroform. This ZnTMP was then demetallated by treatment with dilute HCl. Ruthenium insertion was achieved by refluxing a DMF suspension of Ru_3CO_{12} and $TMPH_2$-zeolite for 1 h. The product was washed with water and methanol, then dried under vacuum overnight at 100°C.

We also attempted to synthesize the fluorinated porphyrin tetrakis-(pentafluorophenyl)porphyrin (PFTPP) encapsulated in zeolite Y. This porphyrin, in which all the hydrogens on the four phenyl rings are replaced by fluorines, is also a known hydrocarbon oxidation catalyst. Under these oxidizing conditions, the fluorinated species are more stable than the TPP species.[123] Because of these advantages, we decided the PFTPP complexes of several metals were worth examining as partial methane oxidation catalysts. The procedure used for the synthesis of the PFTPP/Y is based on the procedure reported earlier for the synthesis of encapsulated TPP species (Quarterly Report No. 3). However, when the pentafluorobenzaldehyde and pyrrole were mixed, an exothermic reaction took place to give a black, tarry solid. This was added to the refluxing acetic acid suspension of zeolite Y, and then the mixture was refluxed further for a few hours. After cooling and filtering, we dissolved away the zeolite by dissolution in concentrated sulfuric acid and then examined this solution by UV-VIS spectroscopy. The spectrum did not display any trace of the chromophore identified with PFTPP. Modifying the reaction procedure by adding pyrrole slowly to a refluxing mixture of zeolite and pentafluorobenzaldehyde also did not give the desired porphyrin.

Cobalt Schiff-base complexes have long been studied as mimics for the oxidation activity of oxygenase enzymes as well as for the oxygen-carrying ability of hemoglobin.[124] We had available to us some encapsulated cobalt Schiff bases from another project, so we examined their potential as partial oxidation catalysts of methane. The catalysts were synthesized by first ion-exchanging the cobalt ions into LZ-Y52 zeolite. The salicylaldehyde derivative and the desired diamine were dissolved in ethanol and mixed with the cobalt zeolite. The mixture was heated to reflux overnight, then cooled and filtered. After the zeolite was air dried, the surface adsorbed metal complexes and metal free Schiff bases were extracted with methylene chloride. Excess cobalt ions were back exchanged with sodium acetate in ethanol. An axial base of 1-methyl imidazole was then added to the zeolite catalysts. We prepared two different Schiff bases: [(1,2-diaminopropylene)bis-salicylideniminato]Co(II), CoSalPn (**1**); and [N,N'-(1,1,2,2-tetramethylethylene)bis-(4-methoxysalicylidenimi-nato)]- Co(II), CoVan4TMen (**2**). Their structures are shown in Figure 17. CoVan4Tmen is sterically hindered compared to CoSalPn. Metal loading is 0.7% in CoSalPn/Y and 1.5% in CoVan4TMen/Y.

We also synthesized catalysts for the partial oxidation of methane by supporting tetrasulfophthalocyanines (TSPC) on magnesia (MgO). Magnesia as a support is of great interest because it has been shown to be an active support in the high temperature partial oxidation of methane to give C_2 hydrocarbons. Tetrasulfophthalocyanines were chosen so that the acidic

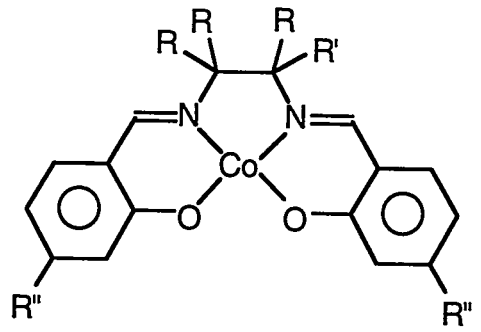

1. CoSalPn: R = H, R' = Ch_3, R" = H
2. $CoVan_4Tmen$: R = R' = CH_3, R" = OCH_3

RM-2678-68

Figure 17. Structure of cobalt Schiff-bases.

sulfonic substituents on the phthalocyanine nucleus would enhance the binding of the metal complex to the basic magnesia support. The first step in the synthesis of the MgO anchored complexes was the synthesis of the individual metal TSPC complexes. These were prepared by the reaction of monosodium-4-sulfophthalic acid, urea, ammonium chloride, and metal salt in the presence of catalytic amounts of ammonium molybdate at 180°C.[122] The metal compounds initially used were $CoCl_2$, $FeCl_2$, $MnSO_4$, $CuCl_2$, $Ru_3(CO)_{12}$, and $Mo(CO)_6$. At a later date, complexes with $PtCl_2$ and $NiCl_2$ were synthesized. The acid forms of the complexes were obtained by treating these complexes with 2N HCl. These complexes were then dissolved in DMF and added to the MgO with stirring. After 2 h, the reaction was filtered and the MgO powders washed with DMF and acetone, then dried overnight at 60°C in a vacuum oven.

The elemental analyses of five of these MgO supported complexes are displayed in Table 12. Assuming that all of the carbon present is associated with the phthalocyanine complex, the Ru and Cu complexes were the most completely metallated on the support. The Fe and Pd systems appeared to have a small excess of unmetallated phthalocyanine present; this demetallation could have occurred during the acidification of the complex, since the complex was used directly after this step. The results for the MoTSPC/MgO system show that a large excess of molybdenum was associated with this system. This abnormally high metal content was most likely due to the presence of molybdenum carbonyl fragments in the MoTSPC used in the deposition reaction. If so, more oxidizing conditions during the acidification step should remove much of this excess molybdenum.

Table 12

ELEMENTAL ANALYSES OF MgO SUPPORTED CATALYSTS

	Experimental				Theoretical[a]			
	%C	%H	%N	%M	%C	%H	%N	%M
FeTSPCMgO	2.26	0.73	0.88	0.24	2.26	0.07	0.66	0.33
RuTSPCMgO	1.95	0.98	0.42	0.45	1.95	0.06	0.57	0.51
PdTSPCMgO	1.05	0.47	0.45	0.18	1.05	0.03	0.31	0.29
CuTSPCMgO	2.37	0.56	0.62	0.37	2.37	0.07	0.69	0.39
MoTSPCMgO	2.36	0.93	0.77	10.21	2.36	0.07	0.69	0.59

[a]Calculated based on carbon content.

We used these results to calculate the concentration of the metal complex per 100 g of magnesia. As shown in Table 13, the concentration for all the complexes except Pd was approximately 0.05 mol/100 g MgO. The Pd loading was about half of this. This difference may be related to the observation that PdTSPC/MgO is the only complex that converts methane into higher hydrocarbons under the reaction conditions (see below).

Table 13

METAL LOADING AND COMPLEX LOADING OF THE MAGNESIUM OXIDE SUPPORTED CATALYSTS

Catalyst	Metal Loading (Wt%)[a]	Complex Loading (mol/100 MgOg)[b]
FeTSPCMgO	0.24	0.052
RuTSPCMgO	0.45	0.047
PdTSPCMgO	0.18	0.026
CuTSPCMgO	0.37	0.054
MoTSPCMgO	10.21	0.057

[a]From elemental analysis.
[b]Moles of complex were calculated based on the carbon weight from the elemental analyses.

TASK 4: TESTING OF METHANE PARTIAL OXIDATION CATALYSTS

We also tried the oxidative coupling reaction of methane reforming [Equations (14) and (15)] because these reactions are thermodynamically favored.[10]

$$nCH_4 + \frac{n}{2} O_2 \longrightarrow C_nH_{2n} + nH_2O \quad (14)$$

$$nCH_4 + \frac{n-1}{2} O_2 \longrightarrow C_nH_{2n+2} + (n-1)H_2O \quad (15)$$

$$nCH_4 \longrightarrow C_nH_{2n+2} + (n-1)H_2 \quad (16)$$

We observed that methane reacts at a lower temperature. With Ru_4ZL as a catalyst, 2.25% of the methane reacted at 200°C, producing mainly hydrogen and carbon dioxide. C_2 hydrocarbons are produced at temperatures of 400°C or higher. This type of methane conversion gives much higher yields than the direct coupling reactions (Table 14). Unfortunately, most of the reacted methane is converted to carbon dioxide and water. The low selectivity to C_2 hydrocarbon, indicates that the noncatalytic gas phase oxidation is a problem in this reaction. Also, these reactions produce significant amounts of hydrogen, which were not expected on the basis of Equations (14) and (15). This result suggested that the methane reacts by a direct coupling path [Equation (16)] after the input oxygen has been consumed. The advantage of this approach is high conversion at low temperature, but the selectivity of C_2 hydrocarbon needs to be improved.

Table 14

OXIDATIVE COUPLING OF METHANE OVER Ru_4ZL[a]

Temperature (°C)	CH_4 Conversion (%)[c]	Selectivity to[b] H_2(%)	CO_2(%)	C_2(%)
200	2.26	16.30	2.33	--[d]
300	3.27	10.61	24.52	–
400	18.87	30.71	61.61	0.44
500	21.09	31.81	54.04	2.32

[a]Reaction conditions: pressure = 50 psig; flow rate = 10 mL/min; CH_4/O_2 = 10.
[b]Selectivities to hydrocarbons are based on carbon number and the amount of methane reacted.
[c]Data are based on four continuous runs within a 1-h period.
[d]Not detected.

We set up a relatively simple isothermal down-flow reactor system to test the oxidation catalysts prepared in Task 3. The system is described in the Experimental section. The catalysts were tested in a glass reactor. All three catalysts (without pyridine treatment) were tested at 200°C under atmospheric pressure. Neither GC nor ^1H NMR spectroscopy detected methanol during a 24-h run. The liquids collected from each run contained water and small amounts of aromatic compounds. We do not know whether the aromatic compounds resulted from decomposition of phthalocyanine or from unreacted organic starting materials that were trapped inside the zeolite pore. The elemental analyses of these catalysts always showed a higher carbon content than is required for phthalocyanine complexes with respect to the metal content. As observed from the elemental analyses, little change in the carbon, hydrogen, and metal content occurred on reaction except in the case of iron phthalocyanine (see Table 15). This result indicates that the metallophthalocyanines are stable under the reaction conditions. In the case of the FePC catalysts, more than 50% of carbon and hydrogen were lost and the percentage of iron increased. Although all three catalysts were treated by the same procedure, a larger amount of organic compounds could have been trapped in the zeolite pores of the FePC catalyst than in the other two cases. This possibility is indicated by an unusually high carbon content in the fresh FePC catalyst.

Table 15

ELEMENTAL ANALYSES OF ZEOLITE CONFINED PHTHALOCYANINE COMPLEXES

		Element Content (wt%)		
Catalyst	**Conditions**	**Carbon**	**Hydrogen**	**Metal**
CoPC	Before reaction	14.53	1.59	1.96
	After reaction	14.49	1.99	2.00
FePC	Before reaction	25.61	1.80	1.19
	After reaction	11.68	0.70	1.60
RuPC	Before reaction	17.35	1.87	1.58
	After reaction	18.15	1.95	1.74

Because glass beads catalyze the oxidation of methane to methanol, we switched to a ss reactor and reexamined the RuPC catalyst. Under the same reaction conditions (flow rate, temperature, pressure, and reaction time), small amounts of methanol, together with water and some unidentified product, were formed. The formation of methanol was confirmed by GC/MS.

No methanol was formed in the absence of RuPC. Blanks run over the zeolite and the Ru exchanged zeolite showed no methanol formation.

We tested all eight zeolite catalysts that were treated with sodium ion for methane oxidation at 375°C under 50 psig pressure. A heated 1/16-in. ss tube (110°C) was added between the reactor and the GC sampling valve. The methane to oxygen feed ratio was 4 and the GHSV was about 2600 h^{-1}. Catalysts were activated under hydrogen flow at 200°C for 2 h before introduction of the methane/oxygen mixture. Thus, the Fe(III) complexes were reduced to Fe(II). When synthesized with $Ru_3(CO)_{12}$, the Ru complexes obtained were coordinated with CO. Activation with hydrogen reductively removed the CO and freed the coordinate site. Other impurities such as water and residue solvent were also removed during this process.

The methane reaction results are averaged from data taken during the 15 to 20 h of the runs and are summarized in Table 16. Three catalysts, RuPCZL, CoTPPZL, and MnTPPZL, showed some reactivity toward the formation of methanol. As shown in Table 16, the RuPCZL gave the highest selectivity to methanol. The methane conversions were generally below 10%. Carbon dioxide and water were always the major products.

Three control experiments were run, using the blank zeolite, ruthenium exchanged zeolite (with triruthenium dodecacarbonyl), and ruthenium tetracarboxyphthalocyanine. The blank zeolite gave essentially no reactivity on methane oxidation. Less than 0.5% of methane was oxidized to carbon dioxide. The ruthenium zeolite produced hydrogen, carbon dioxide, and water with approximately 16% methane conversion. The RuTPPZL and FePCZL also gave hydrogen, a result which suggests that these two catalysts behaved like the simple metal exchanged zeolite. The excess metal ions in these two catalysts were not removed by the reverse ion exchange process, so the production of hydrogen was due to the catalytic ability of the zeolite adsorbed metal particles. We have observed similar results from the ruthenium cluster bonded zeolite. At 400°C and a CH_4/O_2 ratio of 10, Ru4ZL gave 30.7% hydrogen and 61.6% carbon dioxide, with 18.9% methane conversion.

In the absence of the zeolite support, RuTCPC does not convert methane to the desired product. Only 1.7% of the methane was consumed, and the products were carbon dioxide and water. A slight excess of water was produced as a result of decomposition of the peripheral substituent (-COOH). The choice of TCPC was made simply because this compound was available in our laboratory.

Table 16

ACTIVITY OF METHANE OXIDATION CATALYSTS[a]

	%Conversion			%Selectivity	
Catalyst	CH_4	H_2	CO_2	H_2O	CH_3OH
Zeolite	0.5	–	100	–	–
RuZL	15.9	45	100	100	–
RuTCPC	1.7	–	100	206	–
CoPCZL	6.3	–	100	100	–
FePCZL	18.2	1.2	100	42	–
RuPCZL	4.8	–	87	1	11.3
MnPCZL	9.6	–	80	65	–
CoTPPZL	1.9	–	94	120	5.8
FeTPPZL	1.9	–	100	73	–
RuTPPZL	8.4	50	99	146	–
MnTPPZL	1.8	–	95	126	3.5

[a]Reaction conditions: temperature = 375°C, pressure = 50 psig, CH4/O2 = 4, GHSV = 2600 h-1.

Some of the catalysts were also tested at higher temperatures under the same conditions. The results were averaged from 4-h runs and are summarized in Table 17. Methane conversions were generally increased. Again, only RuPCZL and CoPCZL showed some reactivity for methanol formation, and the yields were significantly decreased. These results suggest that these reactions are better run at lower temperatures. Also, at high temperatures the ligand decomposed. Table 18 lists the elemental analysis results after the catalysts were reacted with methane and oxygen at 450°C. The carbon contents decreased to less than 0.2% except for the RuTPPZL, where C remained approximately the same. RuTPP may be more stable than the other complexes. In the case of CoPCZL, a mixture of hydrocarbons was released during the first hour of reaction at 375°C.

Table 17

ACTIVITY OF METHANE OXIDATION CATALYST

Catalyst	Temp. (°C)	%Conversion			%Selectivity		
		CH_4	O_2	H_2	CO_2	H_2O	CH_3OH
RuZL	375	15.9	99.0	45.0	100.0	100.0	–
	500	20.8	99.0	110.0	89.3	–	–
FePCZL	375	18.2	53.9	1.2	100.0	42.5	0.0
	500	22.7	87.2	15.9	100.0	45.0	–
RuPCZL	375	4.8	14.5	–	87.5	0.5	11.3
	450	9.0	99.6	–	96.7	0.5	3.3
CoTPPZL	375	1.9	15.1	–	94.3	119.7	5.8
	450	3.3	56.1	–	98.0	126.2	2.0
FeTPPZL	375	1.9	15.1	–	100.0	–	–
	450	6.1	32.8	–	100.0	65.1	–

Table 18

ELEMENTAL ANALYSIS OF METHANE OXIDATION CATALYSTS BEFORE AND AFTER REACTION WITH METHANE AND OXYGEN AT 450°C

Catalyst[a]	%Carbon	%Hydrogen	%Nitrogen	%Metal
FePCZl-b	8.06	1.51	1.98	4.15
-c	0.10	0.46	<0.05	3.46
RuPCZL-b	2.30	.68	0.42	0.97
-c	0.13	1.00	0.10	0.89
CoTPPZL-b	2.36	1.01	0.41	0.15
-c	0.19	0.47	0.26	0.20
FeTPPZL-b	2.36	1.04	0.48	4.04
-c	0.20	0.69	<0.10	4.03
RuTPPZL-b	2.46	1.13	0.52	0.13
-c	2.13	0.99	0.32	0.14

[a]PC = phthalocyanine, TPP = tetraphenylporphyrin, ZL = zeolite.
[b]Before reaction.
[c]After reaction of methane and oxygen at 450°C.

We tested the FePC and RuPC catalysts for methane oxidation using the reactor system described in Quarterly Report No. 2. The catalysts were activated under hydrogen flow at 200°C for 2 h before the mixture of methane/oxygen (2:1) was added. The product mixture was directed via heated ss tubing (110°C) to a GC sampling valve. No reactivity was observed on either catalyst at 200°C. At 400°C, RuPC showed some methane conversion. Most of the oxygen was consumed and approximately 20% of the methane was converted. Unexpectedly, the product mixture contained a large amount of hydrogen and some hydro-carbons, including ethylene, ethane, propane and propylene. Water was the only oxygen-containing product. Methanol was not detected by the GC. It is possible that the methanol production rate was too slow to be detected. An alternative explanation is that the methanol formed underwent a secondary reaction to give the hydrocarbons. Catalytic cracking of methanol to ethylene and propylene by zeolite catalysts has been observed.

The ligand decomposition results point out that our previous test results on RuPCZL were incorrectly interpreted. We reported in Monthly Report No. 8 that the crude RuPCZL gave C_2 and C_3 hydrocarbon products during a 2 to 4-h run at a temperature range from 300° to 500°C. It is now clear that these hydrocarbons were due to the decomposition of the ligand rather than true products.

CONCLUSIONS AND RECOMENDATIONS

Despite considerable research, oxidative coupling routes to utilization of methane have not proven feasible. In this study we have explored two alternatives: the direct dehydrocoupling of methane to higher hydrocarbons and hydrogen and direct oxidation of methane to methanol. The dehydrocoupling route resulted in up to 50% selectivity to higher hydrocarbons at 6% methane conversion. The direct oxidation route gives up to 11% selectivity to methanol at 5% methane conversion.

Two recent literature reports of reactions similar to those described here are worth noting: methane oxidative coupling has been reported in a simulated counter current moving-bed chromatographic reactor to give C_2 yields of greater than 50%.[17] High-yield oxidation of methane to methanol has also been reported.[38,39] Our recommendation is that the DOE conduct process economic analysis of these two reports to determine if either is commercially viable.

REFERENCES

1. M. E. Dry and J. C. Hoogendoorn, Catal. Rev. **1981**, *23*, 265.

2. D. Hebdon and H.J.F. Stroud, "Coal Gasification Process," Chapter 24 in *Chemistry of Coal Utilization*, M. A. Elliot, Ed. (John Wiley & Sons, New York, **1981**), p. 1602.

3. M. E. Dry, "The Fischer-Tropsch Synthesis," in *Catalysis Science and Technology*, J. B. Anderson and M. Boudart, Eds. (Springer-Verlag, Berlin, **1981**), p. 159.

4. D. L. King, J. A. Cusumano, and R. L. Garten, Catal. Rev. **1981**, *23*, 203.

5. D. McMillen and D. Golden, Annu. Rev. Phys. Chem. **1982**, *33*, 493-532.

6. J. Cox and G. Pilchem, *Thermochemistry of Organic and Organometallic Compounds* (Academic Press, **1970**).

7. a. R. Pitchai and K. Klier, Catal. Rev.-Sci. Eng. **1986**, *28*(1), 13-88.

   b. N. Foster, Appl. Cataly. **1985**, *19*, 1-12.

8. H. Gesser, N. Hunter, and C. Prakash, Chem. Rev. **1985**, *85*(4), 235-244.

9. A. Granada, S. Kavra, and S. Senka, Ind. Eng. Chem. Res. **1987**, *26*, 1901-1905.

10. D. Stull, F. Westrum Jr., and G. Sinke, *The Chemical Thermodynamics of Organic Compounds* (John Wiley & Sons, New York, **1969**).

11. J. Lee and S. Oyami, Catal. Rev.-Sci. Eng. **1988**, *30*(2), 249-280.

12. G. Hutching, M. Scurrell, and J. Woodhouse, Chem. Soc. Rev. **1989**, *18*, 251-283.

13. J. Labinger, Catal. Lett. **1988**, *1*, 371-376.

14. a. J. McCarty, A. McEwen, and M. Quinlan, *New Developments in Selective Oxidation*, C. Centi and F. Trifiro, Eds. (Elsevier, **1990**), pp. 405-415.

    b. J. McCarty, ACS Division, Petroleum Prepr. **1991**, *36*(1), 142-150.

    c. J. McCarty, E. Wachsman, V. Wong, and C. Becker, Proceedings **1992** of the International Gas Research Conference, **1992**, p. 2478.

15. P. Pereira, S. Lee, G. Somorjai, and H. Heinemann, Catal. Lett. **1990**, 255-62.

16. H. Mimoun, A. Robine, S. Bonnaudet, and C. Cameron, Appl. Catal. **1990**, *58*, 269-280.

17. A. Tonkovich, R. Carr, and R. Aris, Science **1993**, *262*, 221-223.

18. D.J.H. Smith, Chimie-Raffinase **1985**, 10.

19. H. Mitchell and R. Waghorne, U.S. Patent No. 4,239,658, **1980**.

20. J. Jones and J. Sofranko, U.S. Patent No. 4,443,645, **1985**.

21. A. Hall and J. McCarroll, U.S. Patent No. 4,695,663, **1987**.

22. O. Gordouin, U.S. Patent No. 4,705,908, **1987**.

23. T. Yamaguchi, A. Kadota, and C. Saito, Chem. Lett. **1988**, 681.

24. R. Wilson Jr., Y.-W. Chan, and B. Posin, Preprint Paper, Am. Chem. Soc., Fuel Chem. Div. **1989**, *34*(4), 1378-1386.

25. P. Broutin, C. Busson, J. Weill, and F. Billaud, *Novel Production Methods for Ethylene, Light Hydrocarbons, and Aromatics*, L. Albright, B. Crynes, and S. Nowak, Eds. (Marcel Dekker, **1972**), pp. 239-258.

26. L. Devries and P. Ryason, U.S. Patent No. 4,507,517, **1985**.

27. O. Bragin, T. Vasina, Ya. Isakov, B. Nefredov, A. Praobrazhenskii, N. Palishkina, and Kh. Minachen, Izv. Akad. Nouk. SSSR, Ser. Khim. **1982**, (4), 954. CA Abstract 97:23370.

28. M. B. Belgued, P. Pareja, A. Amariglio, and N. Amariglio, Nature **1991**, *352*, 789-790.

29. A. Frennet, Catal. Rev. Sci. Eng. **1974**, *10*(10), 37-68.

30. a. Q. Yang, A. Johnson, K. Maynard, and S. Ceyer, J. Am. Chem. Soc. **1989**, *111*, 8748-8749.

    b. J. Beckerle, A. Johnson, Q. Yang, and S. Ceyer, J. Chem. Phys. **1989**, *91*(9), 5756-5777.

    c. J. Beckerle, A. Johnson, and S. Ceyer, J. Chem. Phys. **1990**, *93*(6), 4047-4065.

31. M. Belgued, P. Pareja, A. Amariglio, and H. Amariglio, Nature **1991**, *352*, 789-790.

32. F. Solymosi, A. Erdöhdyi, and J. Cserenyi, Catal. Lett. **1992**, *16*, 399-405.

33. T. Koerts, M. Deelen, and R. van Sauten, J. Catal. **1992**, *138*, 101-114.

34. J. W. Chun and R. Anthony, Ind. Eng. Chem. Res. **1993**, *32*(2), 259-263.

35. A. Shilov, in *Activation and Functionalization of Alkanes*, C. Hill, Ed. (John Wiley & Sons, New York, **1989**), p. 1.

36. E. Gretz, T. Oliver, and A. Sen, J. Am. Chem. Soc. **1987**, *109*, 8109.

37. L. Kao, A. Huston, and A. Sen, J. Am. Chem. Soc. **1991**, *113*, 700.

38. R. Periana, D. Taube, E. Evitt, D. Löffkerm O, Wentrcek, G. Voss, and T. Masuda, Science **1993**, *259*, 340.

39. A. Sen, M. Benvenuto, M. Lin, A. Hutson, and N. Barsickes, J. Am. Chem. Soc. **1994**, *116*, 998.

40. L. E. Patias and A. Tang, Preprint Paper, Am. Chem. Soc., Div. Fuel Chem. **1988**, *33*, 462.

41. R. E. Corder, E. R. Johnson, J. L. Vega, E. C. Clansen, and J. L. Gaddy, Preprint Paper, Am. Chem. Soc., Div. Fuel Chem. **1988**, *33*, 469.

42. M. J. Ceon and R. E. White, in *Metal Ion Activation of Dioxygen*, T. G. Spiro, Ed. (John Wiley & Sons, New York, **1980**), pp. 73-124.

43. J. T. Groves, in *Metal Ion Activation of Dioxygen*, T. G. Spiro, Ed. (John Wiley & Sons, New York, **1980**), pp 125-162.

44. B. Meunier, Bull. Soc. Chim., France, **1986**, 578.

45. P. Gomez-Romero, N. Casan-Pastor, A. Ben-Hussein, and G. B. Jameson, J. Am. Chem. Soc. **1988**, *110*.

46. J. B. Vincent, J. C. Huffman, G. Christou, Q. Li, M. A. Nanny, D. N. Hendrickson, R. H. Tong, and R. H. Fish, J. Am. Chem. Soc. **1988**, *110*, 6898.

47. J. T. Groves and D. V. Subramanian, J. Am. Chem. Soc. **1984**, *106*, 2177.

48. J. Smegal and C. J. Hill, J. Am. Chem. Soc. **1983**, *105*, 515.

49. T. Z. Nemo and J. T. Groves, J. Am. Chem. Soc. **1983**, *105*, 578b.

50. D. Mansuy, Pure Appl. Chem. **1987**, *59*, 759.

51. B. Meunier, M. E. de Carvalho, O. Bartolini, and M. Momenteau, Inorg. Chem. **1988**, 27, 161.

52. P. Battioni, J. F. Bartoli, P. Leluc, M. Fontecave, and D. Mansuy, Chem. Commun. **1987**, 791.

53. S. Udenfriend, C. T. Clark, J. Axelrod, and B. Brodie, J. Biol. Chem. **1954**, 208.

54. T. Matsuura, Appl. Environ. Microbiol. **1987**, *53*, 2844.

55. G. A. Hamilton, J. Am. Chem. Soc. **1966**, *88*, 5266 and 5269.

56. D.H.R. Barton, J. Boivin, M. Gastiger, J. Morzycki, R. S. Motherwell, W. B. Motherwell, N. Ozbalik, and K. M. Schwartzentyruber, J. Chem. Soc., *Perkin Trans. I* **1986**, 947.

57. K. Ono and J. Katsube, Chem. Pharm. Bull. **1982**, *31*, 1267.

58. K. D. Karlin, Y. Gultneh, J. P. Hutchinson, and J. Zubieta, J. Am. Chem. Soc. **1972**, *104*, 5240.

59. C. Merrill, L. J. Wilson, T. J. Thamarn, T. M. Loehr, N. S. Ferris, and W. H. Woodruff, J. Chem. Soc., *Dalton Trans*. **1984**, 2207.

60. W. Brackmann and Z. Havinga, Rec. Trav. Chim. **1955**, *74*, 2070.

61. E. Daire, M. Mimoun, and L. Saussine, Nouv. J. Chim. **1984**, *8*, 271.

62. E. Kumura and P. Machida, Chem. Commun. **1984**, 449.

63. T.J.C. Collins et al., Chem. Commun. **1987**, 803.

64. K. Srinivasan, P. Michaud, and J. K. Kochi, J. Am. Chem. Soc. **1986**, *108*, 2309.

65. R. C. Prince, G. N. George, J. C. Savas, S. P. Gramer, and R. N. Patel, Biochim. Biophys. Acta **1988**, 1504.

66. A. Ericson, B. Hedman, K. O. Hodgson, J. Green, H. Dalton, J. G. Bentsen, R. H. Beer, and S. J. Lippard, J. Am. Chem. Soc. **1988**, *110*, 2330.

67. R. H. Fish, R. H. Fong, J. B. Vincent, and G. Christon, Chem. Commun. **1988**, 1504.

68. J. A. Shelnutt, F. V. Stohl, and B. Granuff, Preprint Paper, Am. Chem. Soc. Div. Fuel Chem. **1988**, *33*, 479.

69. N. Herron, G. D. Stucky, and C. A. Tolman, Chem. Commun. **1986**, 1521.

70. H. C.. Foley, S.J.D. Cani, K. D. Tau, K. J. Chao, J. H. Onuferko, C. Dybowski, and B. C. Gates, J. Am. Chem. Soc. **1983**, *105*, 3074.

71. T.-N. Huang and J. Schwartz, J. Am. Chem. Soc. **1982**, *104*, 5244.

72. Y. Iwasawa, T. Nakamura, K. Takamutsu, and S. Ogasawara, J. Chem. Soc., *Faraday Trans*. 1, **1980**, *76*, 939.

73. R. L. Burwell, Jr., and A. Brenner, J. Mol. Catal. **1975**, *1*, 77.

74. Y. Iwasawa, J. Mol. Catal. **1982**, *17*, 93.

75. Y. Yermakov, B. Kuznetsov, and A. Startsev, Kinet. Catal. **1977**, *18*, 674.

76. Y. Yermakov, B. Kuznetsov, Kinet. Catal. **1977**, *18*, 955.

77. B. N. Kuznetsov, Y.I. Yermakov, M. Boudart, and J. P. Collman, J. Mol. Catal. **1978**, *4*, 49.

78. Y. I. Yermakov, J. Mol. Catal. **1983**, *21*, 35.

79. M. Ichikawa,Chem. Commun. **1978**, 566.

80. M. Deeba, J. P. Scott, R. Barth, and B. C. Gates, J. Catal. **1981**, *71*, 373.

81. J. M. Basset and A. Choplin, J. Mol. Catal. **1983**, *21*, 95.

82. J. P. Candlin and H. Thomas, *Supported Organometallic Catalysis in Homogeneous Catalyss II*, D. Forster and J. F. Roth, Eds. ACS, WDC, Adv. Chem. Ser. **1974**, *132*, 212-239.

83. Y. I. Yermakov, Catal. Rev.-Sci. Eng. **1976** *13*, 77.

84. Y. I. Yermakov, B. N. Kuznetsov, and V. A. Zakharou, *Catalysis by Supported Complexes*, Vol. 8 of *Studies in Surface Science and Catalysis* (Elsevier, Amsterdam, 1981).

85. B. C. Gates and J. Lieto, Chemtech. **1989**, *10*, 195.

86. B. C. Gates and J. Lieto, Chemtech. **1989**, *23*, 124.

87. B. C. Gates and J. Lieto, Chemtech. **1980**, *10*, 248.

88. D. D. Whitehurst, Chemtech. **1989**, *10*, 44.

89. D. C. Bailey and S. H. Langer, Chem. Rev. **1981**, *81*, 109.

90. M. Kaminsky, K. J. Yoon, G. L. Geoffroy, and M. A. Vannice, J. Catal. **1985**, *91*, 338.

91. R. B. Calvert and J. R. Shapley, J. Am. Chem. Soc. **1977**, *99*, 5225.

92. F. A. Coton and G. Wilkinson, Inorganic Chemistry, Vol. 4 (John Wiley & Sons, New York, **1982**).

93. B. J. Wood, SRI International, U.S. Patent No. 3,770,797,973, 1972 (need year)

94. N. Herron, C. A. Tolman, and G. D. Stuckey,Chem. Commun. **1986**, 1521.

95. K. M. Smith, *Porphyrins and Metalloporphyrins* (Elsevier, Oxford, 1975).

96. F. H. Smith, *Porphyrins and Metalloporphyrins*, Vol. II (CRC Press, Boca Raton, FL, 1983).

97. J. G. McCarty, R. B. Wilson Jr., and B. J. Wood, Final Report on DOE Contract DE-AG22-85PC80016, SRI Project No. 1245, SRI International, Menlo Park, CA 94025, 1988.

98. K. W. Sancier, W. E. Isakson, and H. Wise, Preprint Paper, Am. Chem. Soc., Div. Petr. Chem., **1978**, *13*, 545.

99. R. Snel, Ind. Eng. Chem. Fund. Am. **1985**, *24*, 257.

100. R. D. Gonzales, Appl. Surf. Sci. **1984**, *19*, 181.

101. K. Foger, Catal. Sci. Technol. **1984**, *6*, 227.

102. W. P. McKenna and E. M. Eyring, J. Mol. Catal. **1985**, *29*, 363.

103. Y. Iwasawa and S. Ogasawara, Chem. Lett. **1979**, 1465.

104. B. Rebenstorf, B. Jonson, and R. Larsson, Acta Chem. Scand. **1982**, *36*, 695.

105. Y. Blum and R. M. Laine, Organometallics **1986**, *5*, 2081.

106. A. A. Bhattacharyya, C. C. Nagel, and S. G. Shore, Organometallics **1983**, *2*, 1187.

107. G. L. Geoffroy and W. L. Gladfelter, J. Am. Chem. Soc. **1977**, *99*, 7656.

108. E. W. Abel and S. Moorhouse, J. Chem. Soc., *Dalton Trans*. **1973**, 1706.

109. J. Venter and M. A. Vannice, Appl. Spectros. **1988**, *42*, 1096.

110. S. Vichiyama and B. C. Gates, J. Catal. **1988**, *110*, 388.

111. E. Guglielminotti, Langmuir, **1986**, *2*, 812.

112. V. L. Kuznetsov, A. T. Bell, and Y. I. Yermakov, J. Catal. **1980**, *65*, 374.

113. L. D'Ornelas, A. Theolier, A. Choplin, and J.-M. Basset, Inorg. Chem. **1988**, *27*, 1261.

114. A. Choplin, L. Huang, J.-M. Basset, R. Mathieu, V. Siriwardane, and S. G. Shore, Organometallics **1986**, *5*, 1547.

115. I. Boszovmenyi, S. Dobos, L. Guczi, L. Marko, W. M. Roiff, Z. Schay, L. Takacs, and A. Vizo-Orosz, in *Proceedings 8th International Congress Catalysis*, Vol. 5 (Verlag Chemie, Weinhein, **1984**) p. 183.

116. L. Guczi in *Metal Clusters in Catalysis*, Vol. 29, B. C. Gates, L. Guczi, and H. Knozinger, Eds. (Elsevier, Amsterdam, **1986**) p. 553.

117. L. Guczi, Z. Schay, K. Lazar, A. Vizi, and L. Marko, Surface Sci. **1981**, *106*, 516.

118. S. Dobos, I. Boxzormenyi, J. Mirk, and L. Guczi, Inorg. Chem. Acta. **1986**, *120*, 135-145.

119. K. J. Balkus, Jr., and R. S. Drago, Preprint Papers, Am. Chem. Soc., Polymer Div. **1986**, 346.

120. a. G. Meyer, D. Wohrle, M. Mohl, and G. Schulz-Ekloff, Zeolites **1984**, *4*, 30.

b. S. Fukuzumi, S. Mochizuki, and T. Tanaka, Isr. J. Chem. **1987, 1988**, *28*, 29.

121. N. Herron, J. Coord. Chem. **1988**, *19*, 25.

122. D. H. Busch and J. H. Weber, Inorg. Chem. **1965**, *4*, 469.

123. P. S. Traylor, D. Dolphin, and T. G. Traylor, Chem. Commun. **1984**, 279-280.

124. A. Nishiniga and H. Tomita, J. Mol. Catal. **1980**, *7*, 179.